

# Viscous-inertial waves on the surface of the Sun: modeling, forward and inverse problems

Tram Thi Ngoc Nguyen<sup>1</sup>, Damien Fournier<sup>1</sup>, and Thorsten Hohage<sup>1,2</sup>

<sup>1</sup>Max-Planck Institute for Solar System research, Göttingen, Germany

<sup>2</sup>Institute for Numerical and Applied Mathematics, University of Göttingen, Germany

## Abstract

This paper develops a mathematical framework for studying the newly discovered solar inertial oscillations, offering promising new avenues for exploring the Sun's dynamics. Under the assumption of purely toroidal motions, the stream function of the flow satisfies a fourth-order scalar equation governing inertial waves on the rotating Sun. We prove well-posedness of wave solutions under explicit conditions on differential rotation. Moreover, we study the inverse problem of simultaneously reconstructing viscosity and differential rotation parameters from either complete or partial surface observations. To this end, we verify the tangential cone condition, ensuring the convergence of iterative regularization methods. Numerical experiments employing the Nesterov-Landweber iteration confirm robustness of the reconstruction across different observation schemes and noise levels.

**Key words.** inverse problems, differential equations on manifolds, forth order elliptic differential equations, helioseismology, inertial waves, iterative regularization, tangential cone condition

**Acknowledgement.** Support from Deutsche Forschungsgemeinschaft (DFG, German Research Foundation) through SFB 1456/432680300 Mathematics of Experiment, Project C04 is gratefully acknowledged.

## 1 Introduction

*Helioseismology* is the study of the internal structure and dynamics of the Sun from observations of solar oscillations on the surface. Such inference is primarily done by analyzing the observed pressure wave (p-modes) and has led to many achievements including the determination of the Sun's differential rotation [37]. However, the sensitivity of p-modes decreases with depth exacerbating the ill-posedness of the inversion. It is this ill-posedness that motivates the present article, and its accompanying analysis of regularized recovery of rotation and viscosity on the Sun.

The recent discovery of numerous *inertial modes* on the surface of the Sun [15] opens new possibilities for helioseismology. Inertial oscillations, whose frequencies are in the range of hundreds of nHz, are caused by the Coriolis force, exhibiting periodic behavior on the timescale of the solar rotation cycle. As a consequence, these modes require very long observation time to be identified. Indeed, their discovery relies on 10 years of data acquisition by the Helioseismic and Magnetic Imager on board the Solar Dynamics Observatory [34]. As many of these modes have maximum energy at the base of the convection zone [15], i.e., at a depth of about 0.71 solar radii, their study promises to give new insight into the dynamics of the deeper layers of the Sun. We will use these newly discovered waves as data of the inversion process.

Most of the observed modes are quasi-toroidal, i.e. almost divergence-free, with very small radial velocity component, giving rise to the use of a 2D model for inertial waves on a rotating sphere. In this framework, we can reduce the vectorial wave equation into a scalar equation employing a *stream function*, the divergence-free component of the Helmholtz decomposition of the flow. This idea was proposed in [40] and extended in [7] to take into account viscous stress, an important component in solar applications [12].

Inspired by these works, we will model the propagation of inertial-viscous waves on the surface of the rotating Sun by the stream function. The vectorial motion equation driven by Coriolis force and viscous stress will be turned into a fourth-order scalar equation in a low-dimensional setting. Moreover, we derive the *separated* equations for each longitudinal-wavenumber  $m$  with realistic and physical meaningful  $m$ -dependent boundary conditions; this serves as the underlying model for the inverse parameter identification problem.

The problem of solar inversion using inertial waves is completely novel as these modes have been discovered only recently [15]. Here, we take a first step towards recovering the surface differential rotation and the viscosity from dopplergrams. Doppler data are usually not used directly in helioseismology due to the high level of convective noise; indeed, solar excitations can be viewed as random turbulence, resulting in random oscillations. However, some inertial modes have been detected directly in the Doppler signal [14] motivating this study using direct measurements of inertial waves as input data.

Helioseismology predominantly solves linear inverse problem, under the assumption that perturbations are relatively small, as it is the case, for example, for meridional flows [13]. However, for parameters such as viscosity, where no suitable initial guess is available, this linearization assumption may no longer be valid. Here, following a related approach for pressure waves and correlation data in [27], we solve the nonlinear inversion for rotation and viscosity using inertial waves and iterative regularization reconstruction methods.

**Contributions.** This article provides a complete treatment – modelling, forward problem and inverse problem – for the newly observed inertial waves on the Sun:

After a rigorous derivation of the forward model already used in [12], we prove existence, uniqueness and stability of both, the full and separated the inertial wave equations. This well-posedness is derived under explicit conditions on the relative

smallness of variations of the the latitudinal-dependent rotation compared to the product of the frequency and the third power of the viscous parameter. In passing, these results also allow us to apply analytic Fredholm theory, providing mathematical foundations to the recent study of inertial modes. The results of our analysis, both on the conditions for uniqueness and on the isolated occurrence of inertial modes, agree with state-of-the-art interpretations in *inertial mode helioseismology*.

For the inverse problem of the simultaneous identification of viscosity and differential rotation, we lay out foundations of iterative regularization methods by characterizing adjoint operators on a continuous level. Crucially, we provide convergence guarantees for these methods – for full and, to a certain extent, also for restricted observations. We achieve this by establishing the important *tangential cone condition* via a lifted regularity strategy, accounting for realistic  $L^2$ -measurements.

**Structure.** Section 2 introduces the modeling framework for inertial oscillations and outlines different observation strategies for solar data. The well-posedness and regularity of the resulting wave solutions are derived in Section 3. Section 4 addresses the inverse problem for viscosity and differential rotation, including sensitivity analysis and derivation of associated adjoint operators. In Section 5, we establish convergence guarantees of iterative reconstruction schemes by verifying the tangential cone condition. Finally, Section 6 presents numerical reconstruction results under different scenarios, and Section 7 concludes our findings with a summary and an outlook on future research directions.

## 2 Model and observation of inertial waves

### 2.1 Reduced-order modeling of inertial waves

In this section, we derive a physical model for dynamics of waves in the presence of latitudinal differential rotation and eddy viscosity on the Sun in a rotating frame.

**Linearized Navier Stokes equations.** We begin with the equation of motion (momentum equation), in which the dynamics of a moving particle of density  $\rho$  in an incompressible fluid is subject to linear viscous stress  $\boldsymbol{\tau}$  with viscosity  $\gamma$ , acoustic pressure  $p$ , gravity  $\mathbf{g}$ , and external source  $\mathbf{f}$ :

$$\rho \left( \frac{\partial \mathbf{v}}{\partial t} + \nabla_{\mathbf{v}} \mathbf{v} + 2\boldsymbol{\Omega}_{\text{ref}} \times \mathbf{v} \right) = \text{div}(\rho\gamma\boldsymbol{\tau}) - \text{grad } p + \rho\mathbf{g} + \rho\mathbf{f}, \quad (1a)$$

$$\boldsymbol{\tau} := \text{grad } \mathbf{v} + (\text{grad } \mathbf{v})^\top.$$

Here,  $\mathbf{v} = \mathbf{v}(\mathbf{r}, t) \in \mathbb{R}^3$  is the vector velocity of a particle at position  $\mathbf{r} \in \mathbb{R}^3$  and time  $t \in (0, T)$ , while  $\nabla_{\mathbf{v}} := \sum_{i=1}^3 v_i \frac{\partial}{\partial x_i}$  applies componentwise. We work in the frame rotating at the angular frequency  $\Omega_{\text{ref}}$  around a fixed axis  $\hat{\mathbf{a}}$  and set  $\boldsymbol{\Omega}_{\text{ref}} = \Omega_{\text{ref}} \hat{\mathbf{a}}$ . Equation (1a) corresponds to the Navier-Stokes equation in a rotating frame. The fictitious force ( $2\boldsymbol{\Omega}_{\text{ref}} \times \mathbf{v}$ ) is the inertial Coriolis force resulting from the transformation between the fixed and the rotating frame. The other additional fictitious forces,

Euler force  $\rho \left( \frac{d\boldsymbol{\Omega}_{\text{ref}}}{dt} \times \mathbf{r} \right)$  and centrifugal force  $\rho \boldsymbol{\Omega}_{\text{ref}} \times (\boldsymbol{\Omega}_{\text{ref}} \times \mathbf{r})$ , are ignored as  $\boldsymbol{\Omega}_{\text{ref}}$  is uniform in time and assumed to be small. For solar applications, one usually chooses the Carrington frame as reference frame with the angular velocity  $\boldsymbol{\Omega}_{\text{ref}} = 14.7^{\circ}/\text{day}$  and the rotation axis  $\mathbf{e}_z = [0, 0, 1]^{\top}$ . Equation (1a) is complemented by the continuity equation (conservation of mass):

$$\frac{\partial \rho}{\partial t} + \text{div}(\rho \mathbf{v}) = 0. \quad (1b)$$

We linearize Eqs. (1) around a stationary background (unperturbed, equilibrium, mean) medium characterized by  $\mathbf{u}_0$ ,  $p_0$ ,  $\rho_0$ , and  $\mathbf{g}_0$  such that

$$\begin{aligned} \mathbf{v}(\mathbf{r}, t) &= \mathbf{u}_0(\mathbf{r}) + \mathbf{u}(\mathbf{r}, t), & \rho(\mathbf{r}, t) &= \rho_0(\mathbf{r}) + \rho'(\mathbf{r}, t), \\ p(\mathbf{r}, t) &= p_0(\mathbf{r}) + p'(\mathbf{r}, t), & \mathbf{g}(\mathbf{r}, t) &= \mathbf{g}_0(\mathbf{r}) + \mathbf{g}'(\mathbf{r}, t), \end{aligned}$$

where  $\mathbf{u}$  is the (perturbed) wave velocity, and  $\mathbf{u}_0(\mathbf{r}) := (\boldsymbol{\Omega}(\mathbf{r}) - \boldsymbol{\Omega}_{\text{ref}}) \times \mathbf{r}$  is assumed to be a differential rotation field with angular velocity  $\boldsymbol{\Omega}(\mathbf{r}) = \Omega(r, \theta) \mathbf{e}_z$  depending only on radius  $r$  and colatitude  $\theta$  in spherical coordinates  $[r; \theta; \phi] \in [0, \infty) \times [0, \pi) \times [0, 2\pi)$ . We assume that the background medium solves the second-order quasilinear elliptic boundary value problem

$$\begin{aligned} -\text{div} \left( \gamma \rho_0 \left( \mathbf{grad} \mathbf{u}_0 + (\mathbf{grad} \mathbf{u}_0)^{\top} \right) \right) + \rho_0 \nabla_{\mathbf{u}_0} \mathbf{u}_0 + 2\rho_0 \boldsymbol{\Omega}_{\text{ref}} \times \mathbf{u}_0 \\ = -\mathbf{grad} p_0 + \rho_0 \mathbf{g}_0, \end{aligned} \quad (2a)$$

$$\text{div}(\rho_0 \mathbf{u}_0) = 0. \quad (2b)$$

The background gravity force derives from a potential  $\mathbf{g}_0 = -\nabla \Phi_0$  that satisfies the Poisson equation  $\Delta \Phi_0 = 4\pi G \rho_0$ , where  $G$  is the gravitational constant. To construct such a background model for the Sun, it is usually assumed that the background flows are weak and the background medium is built from the hydrostatic equilibrium, that is  $\mathbf{grad} p_0 = \rho_0 \mathbf{g}_0$ . This assumption leads to background coefficients that depend only on depth and are given by standard solar models such as model S [8]. Starting from a radial model for density, it is possible to solve Poisson equation to obtain the gravitational potential and deduce the background pressure.

*Assumption: Waves have small amplitude in comparison to the mean flow, i.e.  $|\mathbf{u}| \ll |\mathbf{u}_0|$ . Moreover, the anelastic approximation  $\rho' \approx 0$  and the Cowling approximation  $\mathbf{g}' \approx 0$  (see [9]) hold true.*

The anelastic approximation is justified if the flow speed is significantly smaller than the sound speed, which is adequate for inertial modes – a few meters per second versus kilometers per second for the surface sound speed. The system (1) thus becomes

$$\rho_0 \left( \frac{\partial \mathbf{u}}{\partial t} + \nabla_{\mathbf{u}_0} \mathbf{u} + \nabla_{\mathbf{u}} \mathbf{u}_0 + 2\boldsymbol{\Omega}_{\text{ref}} \times \mathbf{u} \right) = -\mathbf{grad} p' + \text{div} [\rho_0 \gamma \boldsymbol{\tau}'] + \rho_0 \mathbf{f}, \quad (3a)$$

$$\text{div}(\rho_0 \mathbf{u}) = 0, \quad (3b)$$

where  $\boldsymbol{\tau}' := \mathbf{grad} \mathbf{u} + (\mathbf{grad} \mathbf{u})^{\top}$ .

The flow field  $\mathbf{u}_0$ , equivalently  $\Omega$ , and the viscosity  $\gamma$  will be the quantities of interest in the inverse problem.

**Stratified equations.** We first rewrite the left-hand side of (3a) in spherical coordinates, i.e. in terms of the components  $u_r, u_\theta, u_\phi$  of the expansion  $\mathbf{u} = u_r \mathbf{e}_r + u_\theta \mathbf{e}_\theta + u_\phi \mathbf{e}_\phi$  into the local orthonormal basis vectors  $\mathbf{e}_r, \mathbf{e}_\theta$ , and  $\mathbf{e}_\phi$  as defined in the appendix A. Noting that  $\mathbf{u}_0 = (\Omega(r, \theta) - \Omega_{\text{ref}}) \sin \theta \mathbf{e}_\phi$  and using the identities

$$\begin{aligned}\boldsymbol{\Omega} \times \mathbf{u} &= \Omega (-\sin \theta u_\phi \mathbf{e}_r - \cos \theta u_\phi \mathbf{e}_\theta + (\sin \theta u_r + \cos \theta u_\theta) \mathbf{e}_\phi), \\ \nabla_{\mathbf{u}_0} \mathbf{u} &= (\Omega - \Omega_{\text{ref}})(r, \theta) \frac{\partial \mathbf{u}}{\partial \phi} + (\boldsymbol{\Omega} - \boldsymbol{\Omega}_{\text{ref}}) \times \mathbf{u}, \\ \nabla_{\mathbf{u}} \mathbf{u}_0 &= (\boldsymbol{\Omega} - \boldsymbol{\Omega}_{\text{ref}}) \times \mathbf{u} + \left( \frac{\partial \Omega}{\partial r}(r, \theta) r \sin \theta u_r + \frac{\partial \Omega}{\partial \theta}(r, \theta) \sin \theta u_\theta \right) \mathbf{e}_\phi,\end{aligned}$$

we obtain

$$\begin{aligned}& [\mathbf{e}_r; \mathbf{e}_\theta; \mathbf{e}_\phi]^\top \left( \frac{\partial \mathbf{u}}{\partial t} + \nabla_{\mathbf{u}_0} \mathbf{u} + \nabla_{\mathbf{u}} \mathbf{u}_0 + 2\boldsymbol{\Omega}_{\text{ref}} \times \mathbf{u} \right) \\ &= \mathbf{D}_t \begin{bmatrix} u_r \\ u_\theta \\ u_\phi \end{bmatrix} + \begin{bmatrix} 0 & 0 & -2\Omega \sin \theta \\ 0 & 0 & -2\Omega \cos \theta \\ (2\Omega \sin \theta + \frac{\partial \Omega}{\partial r} r \sin \theta) & (2\Omega \cos \theta + \frac{\partial \Omega}{\partial \theta} \sin \theta) & 0 \end{bmatrix} \begin{bmatrix} u_r \\ u_\theta \\ u_\phi \end{bmatrix}, \quad (4)\end{aligned}$$

where  $\mathbf{D}_t := \frac{\partial}{\partial t} + (\Omega - \Omega_{\text{ref}}) \frac{\partial}{\partial \phi}$  is the *material derivative*.

We now introduce the  $3 \times 2$ -matrix  $\mathbf{R}(\mathbf{r}) := [\mathbf{e}_\theta(\mathbf{r}), \mathbf{e}_\phi(\mathbf{r})]$ . Then multiplication by the  $3 \times 3$  matrix  $\mathbf{R}(\mathbf{r})\mathbf{R}(\mathbf{r})^\top$  is the projection onto the tangential subspace and equivalent to the application of  $-\mathbf{r} \times \mathbf{r} \times$ . By applying  $-\mathbf{r} \times \mathbf{r} \times$  to (3a), we wish to obtain an approximate equation for the horizontal velocity components  $\mathbf{u}_h(\mathbf{r}) := -\mathbf{r} \times \mathbf{r} \times \mathbf{u}(\mathbf{r})$  given by  $\mathbf{u}_h = \mathbf{R}(\mathbf{r})\mathbf{R}(\mathbf{r})^\top \mathbf{u} = u_\theta \mathbf{e}_\theta + u_\phi \mathbf{e}_\phi$ . To this end, we need the following assumption:

*Assumption: Viscosity and density are radially symmetric, i.e.  $\gamma = \gamma(r)$  and  $\rho_0 = \rho_0(r)$ . The fluid is strongly stratified in the sense that the radial motion  $u_r$  and its derivatives are small compared to the horizontal components  $u_\phi, u_\theta$ .*

Due to this assumption, we can neglect the first column of the matrix in Eq. (4), and the application of  $\mathbf{R}(\mathbf{r})\mathbf{R}(\mathbf{r})^\top$  “kills” the first row of this matrix (the first element of the vector in (4) may be balanced by  $\frac{\partial p'}{\partial r}$ ). Therefore, we are left with the matrix

$$\mathbf{M}(\mathbf{r}) := \mathbf{R}(\mathbf{r}) \begin{bmatrix} 0 & -2\Omega(r, \theta) \cos \theta \\ 2\Omega(r, \theta) \cos \theta + \frac{\partial \Omega}{\partial \theta}(r, \theta) \sin \theta & 0 \end{bmatrix} \mathbf{R}(\mathbf{r})^\top$$

and obtain the following system of equations for the tangential vector field  $\mathbf{u}_h$  on  $r\mathbb{S}^2$  for a fixed  $r > 0$  with right hand side  $\mathbf{f}_h := \mathbf{R}\mathbf{R}^\top \mathbf{f}$ :

$$-\rho_0 \gamma \boldsymbol{\Delta}_h \mathbf{u}_h + \rho_0 \mathbf{D}_t \mathbf{u}_h + \rho_0 \mathbf{M} \mathbf{u}_h = \mathbf{grad}_h p' + \rho_0 \mathbf{f}_h, \quad (5a)$$

$$\text{div}_h \mathbf{u}_h = 0. \quad (5b)$$

employing the fact  $\mathbf{grad}(\rho_0(\mathbf{grad} \mathbf{u}_h)^\top) = \mathbf{grad}_h(\rho_0 \text{div}_h \mathbf{u}_h) = 0$  due to (5b).

Physically, the assumption of small radial motions is motivated by an identification of the observed inertial modes from [15] as the eigenvalues of the 3D linearized equations of momentum, mass and energy [5]. In this setup, the radial velocities

of the eigenfunctions are small compared to the horizontal ones for most of the observed modes. This is also the case in nonlinear simulations of rotating convection in a spherical shell [6]. This assumption could possibly be justify mathematically within an asymptotic analysis as  $r \rightarrow \infty$  or  $\Omega \rightarrow 0$ . This, however, would require to amend the system (3) by an atmospheric model and assumptions on the coefficient functions and is beyond the scope of this paper.

**Reformulation as scalar fourth-order equation.** It follows from the Helmholtz decomposition (49) and Eq. (5b) that there exists a stream function  $\Psi$  such that

$$\rho_0 \mathbf{u}_h = \mathbf{curl}_h \Psi.$$

In order to obtain an equation for  $\Psi$ , we apply  $\mathbf{curl}_h$  to (5a). Noting that  $\mathbf{curl}_h(\rho_0 \mathbf{u}_h) = \mathbf{curl}_h \mathbf{curl}_h \Psi = -\Delta_h \Psi$  and using the identities

$$\begin{aligned} \mathbf{curl}_h \mathbf{D}_t(\rho_0 \mathbf{u}_h) &= -D_t \Delta_h \Psi - \frac{1}{r^2} \frac{\partial \Omega}{\partial \theta} \frac{\partial^2 \Psi}{\partial \theta \partial \phi}, \\ \mathbf{curl}_h \rho_0 \gamma \Delta_h \mathbf{u}_h &= -\gamma (\mathbf{curl}_h \mathbf{curl}_h)^2 \Psi = -\gamma \Delta_h^2 \Psi \\ \mathbf{curl}_h \mathbf{M}(\rho_0 \mathbf{u}_h) &= \alpha_\Omega \frac{\partial \Psi}{\partial \phi} + \frac{1}{r^2} \frac{\partial \Omega}{\partial \theta} \frac{\partial^2 \Psi}{\partial \theta \partial \phi}, \quad \alpha_\Omega(\theta) := \frac{1}{r^2 \sin \theta} \frac{d}{d\theta} \left( \frac{1}{\sin \theta} \frac{d}{d\theta} (\Omega(\theta) \sin^2 \theta) \right) \end{aligned} \quad (6)$$

with the analog  $D_t := \frac{\partial}{\partial t} + (\Omega - \Omega_{\text{ref}}) \frac{\partial}{\partial \phi}$  of  $\mathbf{D}_t$ , we arrive at the scalar fourth-order equation

$$\gamma \Delta_h^2 \Psi - D_t \Delta_h \Psi + \alpha_\Omega \frac{\partial \Psi}{\partial \phi} = f \quad (7)$$

with  $f := \rho_0 \mathbf{curl}_h \mathbf{f}_h$ , and  $\alpha_\Omega$  is a linear function of  $\Omega$  as in (6) for convenience.

If we are looking for time-harmonic solutions  $\Psi(t, \mathbf{r}) = \Re(e^{i\omega t} \Psi_\omega(\mathbf{r}))$ , then the space-dependent part has to satisfy the fourth-order elliptic equation

$$\gamma \Delta_h^2 \Psi - \beta_\Omega \Delta_h \frac{\partial \Psi}{\partial \phi} + i\omega \Delta_h \Psi + \alpha_\Omega \frac{\partial \Psi}{\partial \phi} = f \quad (8)$$

with  $\beta_\Omega(\theta) := \Omega(r, \theta) - \Omega_{\text{ref}}$ .

## 2.2 Separated equation as inversion model

Expanding  $\Psi_\omega(\theta, \phi) = \frac{1}{\sqrt{2\pi}} \sum_{m=-\infty}^{\infty} \widehat{\Psi}_{\omega,m}(\theta) e^{im\phi}$  into a Fourier series in azimuth, the coefficients  $\widehat{\Psi}_{\omega,m}$  satisfy the ordinary boundary value problems

$$\begin{cases} \gamma \widehat{\Delta}_m^2 \widehat{\Psi}_{\omega,m}(\theta) + i\omega \widehat{\Delta}_m \widehat{\Psi}_{\omega,m}(\theta) - im\beta_\Omega(\theta) \Delta_m \widehat{\Psi}_{\omega,m}(\theta) + im\alpha_\Omega(\theta) \widehat{\Psi}_{\omega,m}(\theta) = \widehat{f}_m(\theta) \\ (\Gamma_m \widehat{\Psi}_{\omega,m})(\theta) = 0, \quad \theta \in P := \{0, \pi\} \end{cases} \quad (9)$$

with  $\widehat{\Delta}_m$  defined by (54) in Appendix A, and the following boundary value operators derived in Appendix B

$$\Gamma_0 \Psi := \begin{pmatrix} \Psi'|_P \\ \Psi'''|_P \end{pmatrix}, \quad \Gamma_{\pm 1} \Psi := \begin{pmatrix} \Psi|_P \\ \Psi''|_P \end{pmatrix}, \quad \Gamma_m \Psi := \begin{pmatrix} \Psi|_P \\ \Psi'|_P \end{pmatrix}, \quad |m| \geq 2. \quad (10)$$

We remark that this equation reduces to Eq. (2.9) in [40] if  $\gamma = 0$  and to Eq. (8) in [12] if  $\hat{f}_m = 0$ . However, vanishing Cauchy data are imposed at the poles in [12], which for  $|m| \leq 1$  may yield solutions that do not correspond to the unseparated equation (8).

The system (9)-(10) is the underlying model for the parameter inversion problem considered in Section 4. Solving this inverse problem requires measured data, which is the newly discovered inertial waves in this study. The acquisition process will be detailed in the forthcoming section.

### 2.3 Observation of solar oscillations

The basic input of helioseismology are measurements of line-of-sight velocity based on Doppler shifts of certain spectral lines. These so-called dopplergrams acquired since 1996 by ground- or space-based telescopes have high-spatial resolution, of at least  $1000 \times 1000$  pixels, and a temporal cadence of at least 1 minute. A Fourier transform of the dopplergrams data  $v_{\text{dop}}(\theta, \phi, t)$  in longitude  $\phi$  and time  $t$  yields data  $v_{\text{dop}}^{m,\omega}(\theta)$ . Due to the limited data coverage, as only at most half of the Sun is visible at a given time, the transform in  $\phi$  can only be integrated on  $[0, \pi]$  instead of  $[0, 2\pi]$ , leading to a leakage of the signal; see, e.g. the review in [4].

Moreover an operator should be applied to convert the simulated  $\hat{\Psi}$  into  $v_{\text{dop}}$  using for example that  $v_{\text{dop}} = \mathbf{l} \cdot \mathbf{u}$ , where  $\mathbf{l}$  is the line-of-sight vector. On a formal point of view, this could be written as a (linear) operator that transforms  $\Psi$  onto  $v_{\text{dop}}$ . We will not consider this aspect in this article, simply assuming that reprocessed signal  $y^\delta$  is available and described by

$$y^\delta(\theta) = \Psi(\theta) + \text{noise}(\theta) \quad \theta \in I := (0, \pi) \quad \text{or} \quad \theta \in I' := (\epsilon, \pi - \epsilon), \epsilon \geq 0, \quad (11)$$

here  $\delta = \|\text{noise}\|$  denotes the noise level. The case  $\epsilon = 0$  corresponds to full surface coverage, while  $\epsilon > 0$  takes into account that higher latitudes cannot easily be observed due to the line-of-sight projection.

It is usually not possible to work with the Doppler signal directly due to the high level of convective noise. However, some inertial modes of large amplitudes have been directly detected [14], enabling us to consider the recovery of viscosity and rotation from the measurements of  $y^\delta$ .

## 3 Inertial waves on the manifold $r\mathbb{S}^2$

We first show the well-posedness of Eq. (8) associated to the differential operator

$$\mathbf{B}(\Psi) := \gamma \Delta_{\text{h}}^2 \Psi + i\omega \Delta_{\text{h}} \Psi - \beta_\Omega \Delta_{\text{h}} \frac{\partial \Psi}{\partial \phi} + \alpha_\Omega \frac{\partial \Psi}{\partial \phi} \quad (12)$$

with recalling that  $\beta_\Omega(\theta) = \Omega(\theta) - \Omega_{\text{ref}}$  and  $\alpha_\Omega(\theta) = \frac{1}{r^2 \sin \theta} \frac{d}{d\theta} \left( \frac{1}{\sin \theta} \frac{d}{d\theta} (\Omega(\theta) \sin^2 \theta) \right)$ . We will work in the space  $H_\diamond^2(r\mathbb{S}^2)$  of functions in  $H^2(r\mathbb{S}^2)$  with zero mean introduced in the Appendix A.

By partial integration with taking into account symmetry of the bi-Laplacian and Laplacian operators (see Appendix, Lemma 18), the corresponding sesquilinear form  $\mathbf{A} : H_\diamond^2(r\mathbb{S}^2) \times H_\diamond^2(r\mathbb{S}^2) \rightarrow \mathbb{C}$  defined by  $\mathbf{A}[\Psi, \psi] := \langle \mathbf{B}(\Psi), \psi \rangle_{H_\diamond^{-2}, H_\diamond^2}$  is given by

$$\begin{aligned} \mathbf{A}[\Psi, \psi] &= \gamma \langle \Delta_h \Psi, \Delta_h \psi \rangle - i\omega \langle \mathbf{grad}_h \Psi, \mathbf{grad}_h \psi \rangle + (\mathbf{A}^\alpha + \mathbf{A}^\beta)[\Psi, \psi], \\ \mathbf{A}^\alpha[\Psi, \psi] &:= - \left\langle \alpha_\Omega \Psi, \frac{\partial \psi}{\partial \phi} \right\rangle, \quad \mathbf{A}^\beta[\Psi, \psi] := \left\langle \beta_\Omega \Delta_h \Psi, \frac{\partial \psi}{\partial \phi} \right\rangle. \end{aligned} \quad (13)$$

Since the coefficients  $\alpha_\Omega$  and  $\beta_\Omega$  are independent of  $\phi$ , this sesquilinear form is block diagonal with respect to the decomposition  $H_\diamond^2(r\mathbb{S}^2) = \bigoplus_{m \in \mathbb{Z}}^\infty V_m$  with the subspaces

$$V_m := H_\diamond^2(r\mathbb{S}^2; m)$$

introduced in (55). In other words, we have  $\mathbf{A}(\Psi_m, \Psi_n) = 0$  for  $\Psi_m \in V_m, \Psi_n \in V_n$  and  $m \neq n$ . Hence, the restrictions  $\mathbf{A}_m := \mathbf{A}|_{V_m \times V_m}$  fulfill

$$\mathbf{A}(\Psi, \psi) = \sum_{m \in \mathbb{Z}} \mathbf{A}_m(\Psi_m, \psi_m) \quad (14)$$

if  $\Psi = \sum_{m \in \mathbb{Z}} \Psi_m$  and  $\psi = \sum_{m \in \mathbb{Z}} \psi_m$  with  $\Psi_m, \psi_m \in V_m$ . We will also analyze the separated sesquilinear forms given by

$$\begin{aligned} \mathbf{A}_m[\Psi_m, \psi_m] & \quad (15) \\ &= \gamma \langle \Delta_m \Psi_m, \Delta_m \psi_m \rangle - i\omega \langle \mathbf{grad}_h \Psi_m, \mathbf{grad}_h \psi_m \rangle + (\mathbf{A}_m^\alpha + \mathbf{A}_m^\beta)[\Psi_m, \psi_m], \\ \mathbf{A}_m^\alpha[\Psi_m, \psi_m] &:= im \langle \alpha_\Omega \Psi_m, \psi_m \rangle, \quad \mathbf{A}_m^\beta[\Psi_m, \psi_m] := -im \langle \beta_\Omega \Delta_m \Psi_m, \psi_m \rangle. \end{aligned}$$

with  $\mathbf{A}_m^\alpha, \mathbf{A}_m^\beta : V_m \times V_m \rightarrow \mathbb{C}$  as restrictions of  $\mathbf{A}^\alpha, \mathbf{A}^\beta$  defined in (13).

### 3.1 Boundedness

It is straightforward to show that  $\mathbf{A}^\alpha$  and  $\mathbf{A}_m^\alpha$  are bounded if  $\Omega \in W^{2,\infty}(0, \pi)$ . However, we wish to reduce the regularity assumption on the unknown rotation and only assume

$$\Omega \in H^1(r\mathbb{S}^2; m = 0). \quad (16)$$

Under this reduced regularity assumption, establishing boundedness requires additional technical analysis. For later use in a Gårding inequality, we also provide a bound by a weaker norm. In the following, we will frequently employ continuous embeddings between function spaces  $X, Y$  denoted the embedding constants  $C_{X \rightarrow Y}$ , i.e.,  $\|\cdot\|_Y \leq C_{X \rightarrow Y} \|\cdot\|_X$ .

**Lemma 1.** *If  $\Omega \in C^2([0, \pi])$ , then for any  $m \in \mathbb{Z}$  and  $\Psi_m, \psi_m \in V_m \cap C^\infty(r\mathbb{S}^2)$  we have*

$$\mathbf{A}^\alpha[\Psi_m, \psi_m] = \langle \tilde{\alpha}_\Omega \mathbf{grad}_h \Psi_m, \mathbf{curl}_h \psi_m \rangle \quad (17)$$

where  $\tilde{\alpha}_\Omega(\theta) := \Omega'(\theta) \sin \theta + 2\Omega(\theta) \cos \theta$ . Moreover,

$$|\mathbf{A}^\alpha[\Psi_m, \psi_m]| \leq C \|\Omega\|_{H^1} \|\Psi_m\|_{H^2} \|\psi_m\|_{H^{3/2}} \leq C \|\Omega\|_{H^1} \|\Psi_m\|_{H^2} \|\psi_m\|_{H^2} \quad (18)$$

where  $C := 3C_{H_\diamond^1 \rightarrow L^6} C_{H_\diamond^{1/2} \rightarrow L^3}$ .

Under the regularity assumption (16), the right hand side of (17) has a unique continuous extension to a bounded sesquilinear form on  $H_\diamond^2(r\mathbb{S}^2)$ . And the inequality (18) is satisfied for all  $\Psi, \psi \in H_\diamond^2(r\mathbb{S}^2)$ , that is,

$$|\mathbf{A}^\alpha[\Psi, \psi]| \leq C \|\Omega\|_{H^1} \|\Psi\|_{H^2} \|\psi\|_{H^{3/2}} \leq C \|\Omega\|_{H^1} \|\Psi\|_{H^2} \|\psi\|_{H^2}. \quad (19)$$

*Proof.* Let  $\Psi_m, \psi_m \in V_m \cap C^\infty(r\mathbb{S}^2)$ . Note that  $\alpha_\Omega(\theta) = \frac{1}{r^2 \sin \theta} \frac{d}{d\theta} \tilde{\alpha}_\Omega(\theta)$ . As  $\tilde{\alpha}_\Omega \in C^1([0, \pi])$ ,  $\Psi_0(\theta) \frac{\partial \overline{\psi_0}}{\partial \phi}(\theta) = 0$  and  $\Psi_m(\theta) \frac{\partial \overline{\psi_m}}{\partial \phi}(\theta) = -im\Psi_m(\theta) \overline{\psi_m}(\theta) = 0$  for  $\theta \in \{0, \pi\}$ ,  $m \neq 0$ , we can perform a partial integration in  $\theta$  to obtain

$$\begin{aligned} & \mathbf{A}^\alpha[\Psi_m, \psi_m] \\ &= \int_0^{2\pi} \int_0^\pi \tilde{\alpha}_\Omega \frac{\partial}{\partial \theta} \left( \Psi_m \frac{\overline{\psi_m}}{\partial \phi} \right) d\theta d\phi = \int_0^{2\pi} \int_0^\pi \tilde{\alpha}_\Omega \left( \Psi_m \frac{\partial^2 \overline{\psi_m}}{\partial \phi \partial \theta} + \frac{\partial \Psi_m}{\partial \theta} \frac{\partial \overline{\psi_m}}{\partial \phi} \right) d\theta d\phi \\ &= \int_0^{2\pi} \int_0^\pi \tilde{\alpha}_\Omega \left( -\frac{\partial \Psi_m}{\partial \phi} \frac{\partial \overline{\psi_m}}{\partial \theta} + \frac{\partial \Psi_m}{\partial \theta} \frac{\partial \overline{\psi_m}}{\partial \phi} \right) d\theta d\phi \\ &= \int_{r\mathbb{S}^2} \frac{\tilde{\alpha}_\Omega(\theta)}{r^2 \sin \theta} \left( -\frac{\partial \Psi_m}{\partial \phi} \frac{\partial \overline{\psi_m}}{\partial \theta} + \frac{\partial \Psi_m}{\partial \theta} \frac{\partial \overline{\psi_m}}{\partial \phi} \right) ds, \end{aligned} \quad (20)$$

where in the second line we have performed a further partial integration in  $\phi$ . By using (45), we then achieve (17). Next, the generalized Hölder's inequality

$$\left| \int_{r\mathbb{S}^2} abc ds \right| \leq \|a\|_{L^2} \|b\|_{L^3} \|c\|_{L^6} \quad (21)$$

implies

$$|\mathbf{A}^\alpha[\Psi_m, \psi_m]| \leq \|\tilde{\alpha}_\Omega\|_{L^2} \|\mathbf{grad}_h \Psi_m\|_{L^3} \|\mathbf{grad}_h \psi_m\|_{L^6}.$$

The bound  $\|\tilde{\alpha}_\Omega\|_{L^2} \leq \|\frac{\partial \Omega}{\partial \theta}\|_{L^2} + 2\|\Omega\|_{L^2} \leq 3\|\Omega\|_{H^1}$  together with the continuity of the embeddings  $H^1(r\mathbb{S}^2) \hookrightarrow L^6(r\mathbb{S}^2)$  and  $H^{1/2}(r\mathbb{S}^2) \hookrightarrow L^3(r\mathbb{S}^2)$  in (51b) yields (18).

Since  $\mathbf{A}^\alpha$  separates in  $V_m$  and the spaces  $V_m$  are orthogonal in  $H_\diamond^2(r\mathbb{S}^2)$ , the bound (18) also holds true for finite linear combinations of  $\Psi_m$  and  $\psi_m$  of the form above. The last statement (19) follows from the density of such linear combinations (or even linear combinations of spherical harmonics) in  $H_\diamond^2(r\mathbb{S}^2)$ .  $\square$

**Proposition 2.** *Suppose that  $\Omega$  satisfies (16). Then the sesquilinear form  $\mathbf{A}$  defined by (13) is bounded on  $H_\diamond^2(r\mathbb{S}^2)$ , and the separated bilinear forms  $\mathbf{A}_m$  defined by (15) are bounded on  $V_m$ . Both  $\mathbf{A}$  and  $\mathbf{A}_m$  depend continuously on  $\Omega$  with respect to its  $H^1$ -norm.*

*Proof.* Boundedness of  $\mathbf{A}^\alpha$  has been shown in Lemma 1. For  $\mathbf{A}^\beta$ , we again use the Hölder inequality (21) and the same Sobolev embeddings as above to obtain

$$\begin{aligned} |\mathbf{A}^\beta(\Psi, \psi)| &\leq \|\beta\|_{L^6} \|\Delta_h \Psi\|_{L^2} \|\mathbf{grad}_h \psi\|_{L^3} \\ &\leq C_{H^1 \rightarrow L^6} C_{H^{1/2} \rightarrow L^3} \|\Omega - \Omega_{\text{ref}}\|_{H^1} \|\Psi\|_{H^2} \|\psi\|_{H^{3/2}}. \end{aligned} \quad (22)$$

Boundedness of the first two terms in (13) is obvious, and boundedness of  $\mathbf{A}_m$  follows from that of  $\mathbf{A}$ , using (14) and the pairwise orthogonality of the spaces  $V_m$ .  $\square$

### 3.2 Fredholm property and well-posedness

**Theorem 3.** *Let  $\gamma > 0$  and  $\Omega \in H^1(r\mathbb{S}^2; m = 0)$  as in Proposition 2.*

1. *The differential operator  $\mathbf{B} : H_\diamond^2(r\mathbb{S}^2) \rightarrow H_\diamond^{-2}(r\mathbb{S}^2)$  defined in (12) is Fredholm of index 0.*
2. *Moreover,  $\mathbf{B}$  is boundedly invertible at sufficiently large frequencies satisfying*

$$|\omega| > \frac{4}{\gamma^3} (C_{H_\diamond^1 \rightarrow L^6} C_{H_\diamond^{1/2} \rightarrow L^3})^4 (\|\Omega - \Omega_{\text{ref}}\|_{H^1}^2 + 9\|\Omega\|_{H^1}^2)^2. \quad (23)$$

*Proof. Part 1:* Applying Young's inequality  $ab \leq \frac{2}{\gamma}a^2 + \frac{\gamma}{8}b^2$  to the bounds (18) and (22) on  $|\mathbf{A}^\alpha|$  and  $|\mathbf{A}^\beta|$  yields the following Gårding-type inequality:

$$\begin{aligned} \sqrt{2}|\mathbf{A}[\Psi, \Psi]| &\geq |\Re\{\mathbf{A}[\Psi, \Psi]\}| + |\Im\{\mathbf{A}[\Psi, \Psi]\}| \\ &\geq \gamma\|\Delta_h \Psi\|_{L^2}^2 + |\omega|\|\mathbf{grad}_h \Psi\|_{L^2}^2 - |\mathbf{A}^\alpha[\Psi, \Psi]| - |\mathbf{A}^\beta[\Psi, \Psi]| \\ &\geq \frac{3\gamma}{4}\|\Psi\|_{H_\diamond^2}^2 + |\omega|\|\Psi\|_{H_\diamond^1}^2 - \frac{2}{\gamma}(C_{H_\diamond^1 \rightarrow L^6} C_{H_\diamond^{1/2} \rightarrow L^3})^2 (\|\Omega - \Omega_{\text{ref}}\|_{H_\diamond^1}^2 + 9\|\Omega\|_{H_\diamond^1}^2) \|\Psi\|_{H_\diamond^{3/2}}^2. \end{aligned}$$

Since the embeddings  $H_\diamond^1(r\mathbb{S}^2) \hookrightarrow H_\diamond^2(r\mathbb{S}^2)$  and  $H_\diamond^{3/2}(r\mathbb{S}^2) \hookrightarrow H_\diamond^2(r\mathbb{S}^2)$  are compact,  $\mathbf{B}$  is a Fredholm operator of index 0; see, e.g., [33, Sec. 8.2.4].

*Part 2:* Applying the interpolation inequality  $\|\Psi\|_{H_\diamond^{3/2}}^2 \leq \|\Psi\|_{H_\diamond^1} \|\Psi\|_{H_\diamond^2}$  in the last inequality and then Young's inequality  $ab \leq \frac{1}{\gamma}a^2 + \frac{\gamma}{4}b^2$  yields

$$\begin{aligned} \sqrt{2}|\mathbf{A}[\Psi, \Psi]| &\geq \frac{\gamma}{2}\|\Psi\|_{H_\diamond^2}^2 + \left( |\omega| - \frac{4}{\gamma^3} (C_{H_\diamond^1 \rightarrow L^6} C_{H_\diamond^{1/2} \rightarrow L^3})^4 (\|\Omega - \Omega_{\text{ref}}\|_{H^1}^2 + 9\|\Omega\|_{H^1}^2)^2 \right) \|\Psi\|_{H_\diamond^1}^2. \end{aligned}$$

If  $|\omega|$  satisfies (23), then  $\mathbf{A}$  is coercive, so  $\mathbf{B}$  is boundedly invertible by the Lax-Milgram theorem [11, Section 6.2, Theorem 1].  $\square$

We now indicate the dependence of  $\mathbf{B}$  on the frequency  $\omega$  explicitly by  $\mathbf{B}_\omega$  and also consider complex values of  $\omega$ . This allows us to apply analytic Fredholm theory and study resonances:

**Corollary 4.** *There exists a discrete set  $\Lambda \subset \mathbb{C}$  without accumulation points such that  $\mathbf{B}_\omega$  is boundedly invertible in  $L(H_\diamond^2(r\mathbb{S}^2), H_\diamond^{-2}(r\mathbb{S}^2))$  for  $\omega \in \mathbb{C} \setminus \Lambda$ , and  $\dim \ker \mathbf{B}_\omega \in \mathbb{N}$  for  $\omega \in \Lambda$ .*

The elements of  $\ker \mathbf{B}_\omega$  for  $\omega \in \Lambda$  are called inertial modes and have been studied intensively in [12] and other publications.

*Proof of Corollary 4.* It follows from part 1 in the proof of Theorem 3 that  $\mathbf{C}(\omega) : H^2(r\mathbb{S}^2) \rightarrow H^2(r\mathbb{S}^2)$  defined via  $\mathbf{C}(\omega) := (I - \Delta_h)^{-2} \mathbf{B}_\omega - I$  is a compact operator for all  $\omega \in \mathbb{C}$ . Moreover,  $\omega \mapsto \mathbf{C}(\omega)$  is affinely linear and in particular holomorphic.

Therefore, we are in the framework of the analytic Fredholm theorem (see [33, Thm. 7.92]). Note that  $\mathbf{B}_\omega$  is boundedly invertible if and only if  $I + \mathbf{C}(\omega)$  is boundedly invertible and that the kernels of both operators coincide. The first alternative of this theory, that is  $(I + \mathbf{C}(\omega))^{-1}$  does not exist for any  $\omega \in \mathbb{C}$ , is excluded by the second part of Theorem 3. Therefore, the second alternative holds true and provides the statements of this corollary.  $\square$

### 3.3 Separated equations

Let us summarize some consequences for the separated operators  $\mathbf{B}_m : V_m \rightarrow V_m^* = H_\diamond^{-2}(r\mathbb{S}^2; m)$  defined by

$$\langle \mathbf{B}_m \Psi_m, \psi_m \rangle = \mathbf{A}_m[\Psi_m, \psi_m], \quad \Psi_m, \psi_m \in V_m. \quad (24)$$

**Corollary 5.** *For any parameters  $\omega, \gamma, \Omega$  for which  $\mathbf{B}$  is boundedly invertible, in particular for sufficiently large  $|\omega|$  satisfying (23) as in Theorem 3, the separated operators  $\mathbf{B}_m : V_m \rightarrow V_m^*$  are boundedly invertible for all  $m$ .*

*Proof.* It follows from (14) that  $\|\mathbf{B}_m\| \leq \|\mathbf{B}\|$ , so  $\mathbf{B}_m$  is bounded. If  $\mathbf{B}$  is boundedly invertible, then it follows from (14) and the inf-sup characterization of  $\|\mathbf{B}_m^{-1}\|$  that  $\|\mathbf{B}_m^{-1}\| \leq \|\mathbf{B}^{-1}\|$ , and  $\mathbf{B}_m$  is boundedly invertible as well. This completes the proof.  $\square$

*Remark 6.* Repeating the argument of the proof of Theorem 3, it can also be shown that the separated operators  $\mathbf{B}_m$  are Fredholm of index 0. Moreover, Corollary 4 holds true with  $\mathbf{B}_\omega$  replaced by  $\mathbf{B}_m = \mathbf{B}_{m,\omega}$ .

**Proposition 7** (Uniqueness for small  $\Omega'$ ). *For any  $m \in \mathbb{Z}$  the operator  $\mathbf{B}_m : V_m \rightarrow V_m^*$  is boundedly invertible if the derivative  $\Omega'$  (not necessarily differential rotation  $\Omega$  itself) is small in comparison to the viscosity  $\gamma$ , in the sense that*

$$\|\Omega'\|_{L^2(r\mathbb{S}^2)} \frac{|m|}{r} C_{H_\diamond^2 \rightarrow L_\diamond^3} C_{H_\diamond^1 \rightarrow L_\diamond^6} < \gamma. \quad (25)$$

*Proof.* Since  $\mathbf{A}_m$  is bounded by Proposition 2, the Lax-Milgram lemma reduces the proof to verifying the coercivity of  $\mathbf{A}$ . To this end, we estimate its real part under the smallness condition (25). We will employ the (equivalent) norm  $\|u\|_{H_\diamond^2(r\mathbb{S}^2; m)} := \|\Delta u\|_{L^2(r\mathbb{S}^2)}$  for  $u \in H_\diamond^2(r\mathbb{S}^2; m)$ . As  $\Re \mathbf{A}_m^\alpha[\Psi, \Psi] = 0$ , one obtains

$$\Re \mathbf{A}_m[\Psi, \Psi] = \gamma \|\Delta_m \Psi\|_{L^2(r\mathbb{S}^2)}^2 - \Re(im \langle \beta_\Omega \Delta_m \Psi, \Psi \rangle).$$

Using partial integration, the identity  $\mathbf{grad}_h \beta_\Omega = \frac{1}{r} \Omega' \mathbf{e}_\theta$ , Hölder's inequality (21) and the embeddings (58), we can bound

$$\begin{aligned} & \Re(im \langle \beta_\Omega \Delta_m \Psi, \Psi \rangle) \\ & \leq |m| |\Im \langle \mathbf{grad}_h \Psi, \mathbf{grad}_h(\beta_\Omega \Psi) \rangle| = |m| |\Im \langle \mathbf{grad}_h \Psi, \mathbf{grad}_h(\beta_\Omega) \Psi \rangle| \\ & \leq |m| \|\mathbf{grad}_h \Psi\|_{L^6} \|\mathbf{grad}_h \beta_\Omega\|_{L^2} \|\Psi\|_{L^3} \leq \frac{|m|}{r} C_{H_\diamond^2 \rightarrow L_\diamond^3} C_{H_\diamond^1 \rightarrow L_\diamond^6} \|\Omega'\|_{L^2(r\mathbb{S}^2)} \|\Psi\|_{H_\diamond^2}^2. \end{aligned}$$

Therefore,  $\Re \mathbf{A}_m[\Psi, \Psi] \geq c \|\Delta_m \Psi\|_{L^2(r\mathbb{S}^2)}^2$  with  $c := \gamma - \frac{|m|}{r} C_{H_\diamond^2 \rightarrow L_\diamond^3} C_{H_\diamond^1 \rightarrow L_\diamond^6} \|\Omega'\|_{L^2} > 0$  ensured by the assumption (25). This completes the proof of coercivity.  $\square$

### 3.4 Additional regularity

**Proposition 8** (Lifted regularity). *Let  $m \in \mathbb{Z}$  and suppose that (23) or (25) hold true such that  $\mathbf{B}_m : H_\diamond^2(r\mathbb{S}^2; m) \rightarrow H_\diamond^{-2}(r\mathbb{S}^2; m)$  is boundedly invertible. Further assume that source and rotation have regularity*

$$f_m \in L^2(r\mathbb{S}^2; m), \quad \Omega \in H^2(r\mathbb{S}^2; m = 0). \quad (26)$$

Then the solution  $\Psi_m := \mathbf{B}_m^{-1}f_m$  as well as  $\tilde{\Psi}_m := (\mathbf{B}_m^*)^{-1}f_m$  with the adjoint operator  $\mathbf{B}_m^* : H_\diamond^2(r\mathbb{S}^2; m) \rightarrow H_\diamond^{-2}(r\mathbb{S}^2; m)$  have higher regularity

$$\Psi_m \in H_\diamond^4(r\mathbb{S}^2; m). \quad (27)$$

Moreover, with  $\Psi_m(\theta, \phi) = \hat{\Psi}_m(\theta)e_m(\phi)$ , the boundary values  $\Gamma_m \hat{\Psi}_m$  are well defined for all  $m \neq 0$  and  $\Gamma_m \hat{\Psi}_m = 0$ , and similarly for  $\tilde{\Psi}_m$ .

Finally, the restrictions of  $\mathbf{B}_m$  and  $\mathbf{B}_m^*$  have the forms

$$\left. \begin{aligned} \mathbf{B}_m &= \gamma \Delta_m^2 + i\omega \Delta_m - im\beta_\Omega \Delta_m + im\alpha_\Omega \\ \mathbf{B}_m^* &= \gamma \Delta_m^2 - i\omega \Delta_m + im\Delta_m(\beta_\Omega \cdot) - im\alpha_\Omega \end{aligned} \right\} : H_\diamond^4(r\mathbb{S}^2; m) \rightarrow L^2(r\mathbb{S}^2; m)$$

and they have bounded inverses  $\mathbf{B}_m^{-1}, (\mathbf{B}_m^*)^{-1} : L^2(r\mathbb{S}^2; m) \rightarrow H_\diamond^4(r\mathbb{S}^2; m)$ .

*Proof.* The solution  $\Psi_m \in H_\diamond^2(r\mathbb{S}^2; m)$  satisfies

$$\begin{aligned} \forall \psi_m \in H_\diamond^2(r\mathbb{S}^2; m) : \quad \gamma \langle \Delta_m \Psi_m, \Delta_m \psi_m \rangle &= \langle \tilde{f}_m, \psi_m \rangle \\ \text{with } \tilde{f}_m &:= f_m + i\omega \Delta_m \Psi_m - im\beta_\Omega \Delta_m \Psi_m + im\alpha_\Omega \Psi_m. \end{aligned} \quad (28)$$

We shall claim that  $\tilde{f}_m \in L^2(r\mathbb{S}^2; m)$ . As  $\alpha_\Omega = \Omega'' \sin + 3\Omega' \cot - 2\Omega \sin$ , hence  $\Omega \in H^2(r\mathbb{S}^2; 0)$  implies

$$\begin{aligned} \|\alpha_\Omega \Psi_m\|_{L^2} &\leq \|(\Omega'' - 2\Omega \sin) \Psi_m\|_{L^2} + \left\| 3\Omega' \cos \frac{\Psi_m}{\sin} \right\|_{L^2} \\ &\leq (\|\Omega''\|_{L^2} + 2\|\Omega\|_{L^2}) \|\Psi_m\|_{L^\infty} + 3\|\Omega'\|_{L^4} \|\mathbf{grad}_h \Psi_m\|_{L^4} \end{aligned}$$

with noting that  $\Psi_m/\sin$  is  $\phi$ -component of  $\mathbf{grad}_h \Psi_m$  for  $m \neq 0$ ; for the case  $m = 0$ , the term  $\alpha_\Omega$  does not appear in the equation. Using the embeddings (58) and setting  $C_\alpha := 2C_{H^2 \rightarrow L^\infty} + 3C_{H^1 \rightarrow L^4}^2$ , we obtain

$$\|\alpha_\Omega \Psi_m\|_{L^2} \leq C_\alpha \|\Omega\|_{H^2} \|\Psi_m\|_{H^2}. \quad (29)$$

With this we can derive the following norm bound:

$$\begin{aligned} \|\tilde{f}_m\|_{L^2} &\leq \|f_m\|_{L^2} + |\omega| \|\Psi_m\|_{H^2} + |m| \|\beta_\Omega\|_{L^\infty} \|\Psi_m\|_{H^2} + |m| C_\alpha \|\Omega\|_{H^2} \|\Psi_m\|_{H^2} \\ &\leq \|f_m\|_{L^2} + (|\omega| + |m| (C_{H^2 \rightarrow L^\infty} \|\Omega\|_{H^2} + \|\Omega_{\text{ref}}\|_{L^\infty} + C_\alpha \|\Omega\|_{H^2})) \|\Psi_m\|_{H^2}. \end{aligned}$$

It follows from the isometry property (57) that weak solutions  $\Psi \in H_\diamond^2(r\mathbb{S}^2)$  to the bi-harmonic equation  $\Delta_h^2 \Psi = f$  with  $f \in L^2(r\mathbb{S}^2)$  belong to  $H^4(r\mathbb{S}^2)$ . Due to the separability of  $\Delta_h$ , weak solutions  $\Psi_m \in H_\diamond^2(r\mathbb{S}^2; m)$  to the separated equation  $\Delta_m^2 \Psi_m = \tilde{f}_m$

with  $\tilde{f}_m \in L^2_\diamond(r\mathbb{S}^2)$  also belong to  $H^4_\diamond(r\mathbb{S}^2; m)$  with  $\|\Psi_m\|_{H^4} = \|\tilde{f}_m\|_{L^2}$ . Together with  $\|\Psi_m\|_{H^2} \leq \|\mathbf{B}_m^{-1}\| \|f_m\|_{H^{-2}} \leq \|\mathbf{B}_m^{-1}\| \|f_m\|_{L^2}$  this shows that  $\|\Psi_m\|_{H^4} \leq C\|f\|_{L^2}$ , i.e.,  $\mathbf{B}_m : H^4_\diamond(r\mathbb{S}^2; m) \rightarrow L^2(r\mathbb{S}^2; m)$  is boundedly invertible. The proof of the analogous statement for  $\mathbf{B}_m^*$  only requires a different treatment of the term involving  $\beta_\Omega$ . Here, we use the fact that  $H^2(r\mathbb{S}^2)$  is a Banach algebra (see [2, p. 115] or [3, Thm 1.4]) to show that  $\|\beta_\Omega \Psi_m\|_{H^2} \leq C\|\beta_\Omega\|_{H^2} \|\Psi_m\|_{H^2}$ .

Concerning the boundary values, we use the continuous embedding  $H^4(r\mathbb{S}^2) \hookrightarrow C^2(r\mathbb{S}^2)$  in (51c) and Lemma 17 to show that  $\Gamma_m \hat{\Psi}_m$  is well-defined and vanishes.  $\square$

### 3.5 Well-posedness on the restricted domain

Inspired by the practical measurement scenario in Section 2.3, where only data on the restricted latitude range  $I' = (\epsilon, \pi - \epsilon)$  can be observed, this section derives well-posedness, regularity of the wave operators on this restricted domain. This result will be later employed in Section 5.2 for convergence guarantee of reconstruction method under restricted measurements.

We sketch how an analysis similar to that of Propositions 7 and 8 can be carried out, whose key elements are symmetry of the bi-Laplacian and Laplacian operators and partial integrations. According to Remark 19, symmetry of Laplacian operators on function spaces supported on  $I'$  is guaranteed with homogeneous Cauchy boundary data, i.e.  $\Gamma_2$  in (10).

To this end, we define the following function spaces on  $I'$  with norms inherited from  $H^s(r\mathbb{S}^2; m)$ :

$$\begin{aligned} H^s(I'; m) &:= \{\Psi|_{I'} : \Psi \in H^s(r\mathbb{S}^2; m)\}, s \geq 0, \\ H_0^s(I'; m) &:= \{\Psi|_{I'} : \Psi \in H^s(r\mathbb{S}^2; m), \Psi|_{\partial I'} = \Psi'|_{\partial I'} = 0\}, s \geq 2. \end{aligned} \quad (30)$$

Note that these spaces coincide with the standard Sobolev spaces  $H^s(I')$  and  $H_0^s(I')$  with equivalent norms. Correspondingly, the dual spaces are, respectively, given by  $H_0^{-s}(I'; m) := H^s(I'; m)' = H_0^{-s}(I')$  and  $H^{-s}(I'; m) := H_0^s(I'; m)' = H^{-s}(I')$ , again with equivalent norms.

**Proposition 9** (Well-posedness on  $I'$ ). *Given  $\gamma > 0$ , and  $\Omega \in H^1(r\mathbb{S}^2; m = 0)$  satisfying (23) or (25). Assume for any  $m \in \mathbb{Z}$  the Cauchy boundary condition*

$$\Psi|_{\partial I'} = u_1 \in \mathbb{C}^2 \quad \text{and} \quad \Psi'|_{\partial I'} = u_2 \in \mathbb{C}^2. \quad (31)$$

Let  $u \in C^\infty(I)$  with  $u|_{\partial I'} = u_1$ ,  $u'|_{\partial I'} = u_2$  and  $g := \mathbf{B}_m u$ . We claim:

- (i) The operator  $\mathbf{B}_m : H_0^2(I'; m) \rightarrow H^{-2}(I'; m)$  is boundedly invertible. The wave solution is  $\Psi = \mathbf{B}_m^{-1}(f_m - g) + u \in H^2(I'; m)$ .
- (ii) Furthermore, if  $\Omega \in H^2(r\mathbb{S}^2; m = 0)$  as in Proposition 8, then the linear bounded operator  $\mathbf{B}_m, \mathbf{B}_m^*$  have bounded inverses  $\mathbf{B}_m^{-1}, (\mathbf{B}_m^*)^{-1} : L^2(I'; m) \rightarrow H_0^4(I'; m)$ .

*Proof.* The splitting  $\Psi = \mathbf{B}_m^{-1}(f_m - g) + u$  allows us to study the differential operators  $\mathbf{B}_m$  on the state space  $H_0^2(I'; m)$  with homogeneous boundaries as defined in (30).

Symmetry of the bi-Laplacian and Laplacian operators with homogeneous Cauchy boundary condition (31) shown in Remark 13 enables the sesquilinear form  $\mathbf{A}$  in (13). Next, the integration-by-part (20) in Lemma 1 holds under Cauchy boundary condition, implying boundedness of  $\mathbf{A}$ ,  $\mathbf{A}^\alpha$  as in Proposition 2, and well-posedness of the unseparated equation in the same setting as Theorem 3. Then, for the separated equations, following the proof of Proposition 7, in which the partial integration also holds on the subdomain  $I'$ , we obtain the same uniqueness result.

Concerning the lifted regularity result as in Proposition 8, by setting the auxiliary source  $\tilde{f}_m$  as in (28) and partial integration, we (formally) have  $\gamma \langle \Delta_m^2 \Psi_m, \psi_m \rangle = \gamma \langle \Delta_m \Psi_m, \Delta_m \psi_m \rangle = \langle \tilde{f}_m, \psi_m \rangle$  for all  $\psi_m \in H_0^2(I'; m)$ . Using the fact the weak solutions of the bi-Laplace equations are also strong solutions, one obtains boundedness of the fourth order term  $\|\Delta_m^2 \Psi_m\|_{L^2}$ , given higher regularity of  $\Omega$  and  $f$  as in Proposition 8. Alternatively, one can apply general elliptic regularity results as, e.g., in [38, Sec. 5.3.4].  $\square$

## 4 Inverse problems for viscosity and rotation

### 4.1 Inversion with different observation strategies

In this section, we address the inverse problem of recovering the differential rotation function  $\Omega$  and the viscosity coefficient  $\gamma$  in the separated equations. To achieve this, we require additional information, namely full or partial measurements of the state, as described in Section 2.3:

$$\begin{aligned} L : V_m &\rightarrow Y \\ (L\Psi)(\theta) &:= \Psi(\theta) \end{aligned} \quad Y = \begin{cases} L^2(I, r^2 \sin), & \text{full measurements} \\ L^2(I', r^2 \sin), & \text{partial measurements} \end{cases} \quad (32)$$

with the weighted  $L^2$ -data spaces. We formulate the parameter identification problem within the Hilbert space framework established by the well-posedness results in Sections 3.2-3.3:

$$\gamma \in \mathbb{R}^+, \quad \Omega \in X := H^1(r\mathbb{S}^2, m = 0), \quad \Psi \in V_m := H_\diamond^2(r\mathbb{S}^2; m), \quad y \in Y, \quad (33)$$

By introducing the parameter-to-state map

$$\begin{aligned} S : \mathcal{D}(S) &\rightarrow V_m, \quad \mathcal{D}(S) := \{(\gamma, \Omega) \in \mathbb{R}^+ \cap X : (23) \vee (25)\} \\ S(\gamma, \Omega) &:= \Psi, \quad \text{where } \Psi \text{ is the weak solution to (9)} \end{aligned} \quad (34)$$

together with the measurement operator we can formulate the forward operator  $F$  for the parameter identification as

$$F : \mathcal{D}(S) \rightarrow Y \quad F := L \circ S. \quad (35)$$

Note that  $X$  is the space of real-valued functions, while  $V_m$  and  $Y$  are spaces of complex-valued functions; together, they form Gelfand triples.

## 4.2 Sensitivity and adjoints

Compactness of the embedding  $V_m \hookrightarrow L^2(I, r^2 \sin)$  yields compactness of the measurement operator  $L$ , thus of the forward operator  $F$ . In such cases, the inverse coefficient problem becomes ill-posed, necessitating regularization for stable reconstruction. Given the inherent nonlinearity of the problem, iterative methods such as Landweber-type and Newton-type algorithms are typically employed for reconstruction (see Section 5). For noisy data  $y^\delta \in Y$ , the former is given by

$$p_{k+1} = p_k - F'(p_k)^*(F(p_k) - y^\delta) \quad k \leq K(y^\delta, \delta),$$

where the unknown parameter is  $p := (\gamma, \Omega)$ . The stopping index  $K(y^\delta, \delta)$  serves as the *regularization parameter* and is determined according to the *discrepancy principle*; see Section 6 for further details. This formulation highlights that the main components of iterative gradient-based methods: sensitivity analysis and the derivation of the adjoint; these are the primary focus of this section.

To this end, we will add the dependence on the unknown parameters  $p = (\gamma, \Omega) \in \mathcal{D}(S)$  in parenthesis, i.e.  $\mathbf{B}_m(p) = \mathbf{B}_m : V_m \rightarrow V_m^*$ . Since the mapping  $p \mapsto \mathbf{B}_m(p)$  is affinely linear, its derivative with respect to  $p$  is independent of  $p$  and we can omit it in our notation. Hence, we simply denote the derivative of  $p \mapsto \mathbf{B}_m(p)$  by

$$\mathbf{B}'_m : \mathbb{R} \times X \rightarrow \mathcal{L}(V_m, V_m^*), \quad \mathbf{B}'_m(\delta\gamma, \delta\Omega)\Psi := (\delta\gamma)\Delta_m^2\Psi + im\alpha_{\delta\Omega}\Psi - im(\delta\Omega)\Psi.$$

More precisely,  $\mathbf{B}'_m(\delta\gamma, \delta\Omega)$  is the operator induced by the sesquilinear form  $\mathbf{A}'_m(\delta\gamma, \delta\Omega) : V_m \times V_m \rightarrow \mathbb{C}$  defined by

$$\mathbf{A}'_m(\delta\gamma, \delta\Omega)[\Psi, \psi] := (\delta\gamma) \langle \Delta_m \Psi, \Delta_m \psi \rangle + im(\alpha_{\delta\Omega} - \delta\Omega) \langle \Psi, \psi \rangle.$$

We wish to emphasize that a similar analysis can be carried out for the unseparated equation with obvious modifications.

**Lemma 10** (Sensitivity). *The parameter-to-state map  $S$  in (34) is Fréchet differentiable, and for any  $p \in \mathcal{D}(S)$  and  $\delta p \in \mathbb{R} \times X$  we have*

$$S'[p]\delta p = -\mathbf{B}_m(p)^{-1}\mathbf{B}'_m(\delta p)\Psi \in V_m, \quad (36)$$

where  $\Psi := \mathbf{B}_m(p)^{-1}f$  is the weak solution to the primal equation (9).

*Proof.* The result follows from the differentiability statement in the implicit function theorem (see, e.g., [41, §4.7]) applied to the operator  $G : \mathcal{D}(S) \times V_m \rightarrow V_m^*$ ,  $G(p, \Psi) := \mathbf{B}_m(p)\Psi - f$ . Here, one interprets  $S$  as the implicitly defined function  $G(p, S(p)) = 0$  and employs linearity of  $G$  in the second argument as well as bounded invertibility of  $\mathbf{B}_m(p) : V_m \rightarrow V_m^*$ .  $\square$

Differentiability of  $F$  is straightforward from that of  $S$  and boundedness of the linear measurement operator  $L$  defined in (32). We now derive the adjoint for different observation scenarios.

**Proposition 11** (Adjoint – full observation). *Let  $L = Id$ , thus  $F = S$ . Denote by  $I_X : X^* \rightarrow X$  the Riesz isomorphism between dual spaces.*

*The Hilbert space adjoint of the derivative of  $F$  in (35) is given by*

$$F'[p]^* : Y \rightarrow \mathbb{R} \times X \quad F'[p]^* y = - \begin{bmatrix} 1 & 0 \\ 0 & I_X \end{bmatrix} \Re([\mathbf{B}'_m(\cdot)\Psi]^*(\mathbf{B}_m(p)^{-1})^* y) \quad (37)$$

where  $\Psi := \mathbf{B}_m(p)^{-1} f$  is again the solution to the separated equation (9) and

$$[\mathbf{B}'_m(\cdot)\Psi]^* : V_m \rightarrow \mathbb{R} \times X^*, \quad (\mathbf{B}_m(p)^{-1})^* : V_m^* \rightarrow V_m \quad (38)$$

denotes the Banach space adjoints of  $\mathbf{B}'_m(\cdot)\Psi : \mathbb{R} \times X \rightarrow V_m^*$  and  $\mathbf{B}_m(p)^{-1} : V_m^* \rightarrow V_m$ .

*Proof.* Since the parameter space is real, we impose on  $Y$  the real-valued inner product, the real part of the canonical complex-valued inner product, as

$$(f, g)_Y := (\Re(f), \Re(g))_Y + (\Im(f), \Im(g))_Y = \Re\left((f, g)_Y^{\mathbb{C}}\right).$$

The linearization (37) and Banach space adjoints (38) enable us to deduce

$$\begin{aligned} \left(F'[p]\delta p, y\right)_Y^{\mathbb{C}} &= \left\langle S'[p]\delta p, y \right\rangle_{L^2}^{\mathbb{C}} = - \left\langle \mathbf{B}_m(p)^{-1} \mathbf{B}'_m(\delta p) \Psi, y \right\rangle_{L^2}^{\mathbb{C}} \\ &= - \left\langle \mathbf{B}'_m(\delta p) \Psi, (\mathbf{B}_m(p)^{-1})^* y \right\rangle_{V_m^*, V_m}^{\mathbb{C}} = - \left\langle \delta p, [\mathbf{B}'_m(\cdot)\Psi]^*(\mathbf{B}_m(p)^{-1})^* y \right\rangle_{\mathbb{R} \times X, \mathbb{R} \times X^*}^{\mathbb{C}}. \end{aligned}$$

Then with the real-valued inner product and the Riesz isomorphism  $I_X$ , we arrive at

$$\begin{aligned} \left(F'[p]\delta p, y\right)_Y &= \left\langle \delta p, -\Re([\mathbf{B}'_m(\cdot)\Psi]^*(\mathbf{B}_m(p)^{-1})^* y) \right\rangle_{\mathbb{R} \times X, \mathbb{R} \times X^*} \\ &= \left\langle \delta p, - \begin{bmatrix} 1 & 0 \\ 0 & I_X \end{bmatrix} \Re([\mathbf{B}'_m(\cdot)\Psi]^*(\mathbf{B}_m(p)^{-1})^* y) \right\rangle_{\mathbb{R} \times X}, \end{aligned}$$

in agreement with the expression (37).  $\square$

We next derive the explicit expression for the Hilbert space adjoint (37).

**Corollary 12** (Explicit form). *The adjoint for full observation in Proposition 11 takes the explicit form*

$$F'[\gamma, \Omega]^* y = \begin{bmatrix} \Re\left(\int_0^\pi (\Delta_m^2 \Psi) \bar{z} r^2 \sin(\cdot) ds\right) \\ m I_X \Im\left(\frac{\sin(\cdot)}{r^2} \frac{d}{d\theta} \left(\frac{1}{\sin(\cdot)} \frac{d(\bar{\Psi} z)}{d\theta}\right) - (\Delta_m \bar{\Psi}) z\right) \end{bmatrix} \quad (39)$$

with the adjoint state  $z := (\mathbf{B}_m(p)^{-1})^* y$ .

*Proof.* To compute  $[\mathbf{B}'_m(\cdot)\Psi]^*$ , take  $(\delta\gamma, \delta\Omega) \in \mathbb{R} \times X$  and  $z \in V_m$  and note that

$$\begin{aligned} \langle \mathbf{B}'_m(\delta\gamma, \delta\Omega) \Psi, z \rangle &= \langle \delta\gamma \Delta_m^2 \Psi - im(\delta\Omega) \Delta_m \Psi + im\alpha_{\delta\Omega} \Psi, z \rangle \\ &= \delta\gamma \int_0^\pi (\Delta_m^2 \Psi) \bar{z} r^2 \sin(\cdot) d\theta + \langle \delta\Omega, im(\Delta_m \bar{\Psi}) z \rangle - \langle \alpha_{\delta\Omega}, im \bar{\Psi} z \rangle \end{aligned}$$

To characterize the quantity involving  $\alpha_{\delta\Omega}$ , we may assume w.l.o.g. that  $m \neq 0$  since  $\alpha$  is irrelevant for  $m = 0$ . Using the fact the  $\Psi$  and  $z$  satisfy the boundary conditions  $\Gamma_m(\Psi) = \Gamma_m(z) = 0$  under our regularity assumption on  $\Omega$  according to Proposition 8, we can carry out the following partial integrations:

$$\begin{aligned} & \langle \alpha_{\delta\Omega}, \bar{\Psi}z \rangle \\ &= \int_0^\pi \frac{d}{d\theta} \left( \frac{1}{\sin\theta} \frac{d}{d\theta} (\delta\Omega \sin^2\theta) \right) \Psi \bar{z} d\theta = \int_0^\pi \frac{-1}{\sin\theta} \frac{d}{d\theta} (\delta\Omega \sin^2\theta) \frac{d}{d\theta} (\Psi \bar{z}) d\theta \\ &= \int_0^\pi (\delta\Omega)(\theta) \sin^2\theta \frac{d}{d\theta} \left( \frac{1}{\sin\theta} \frac{d}{d\theta} (\Psi \bar{z}) \right) d\theta = \left\langle \delta\Omega, \frac{\sin}{r^2} \frac{d}{d\theta} \left( \frac{1}{\sin} \frac{d}{d\theta} (\bar{\Psi}z) \right) \right\rangle \end{aligned}$$

Inserting these formulas into (37) yields (39).  $\square$

*Remark 13* (Adjoint for partial and real measurements). Note that the partial observation operator is the restriction operator  $R\Psi := \Psi|_{I'}$ . Its Hilbert space adjoint is obviously the extension-by-zero operator

$$R^* : L^2(I', r^2 \sin) \rightarrow L^2(I, r^2 \sin) \quad R^*\Psi(\theta) := \begin{cases} \Psi(\theta), & \theta \in I', \\ 0, & \theta \in I \setminus I'. \end{cases}$$

The corresponding forward operator is  $F = RS$ , thus  $F'[p]^* = S'[p]^* R^*$  with  $S'[p]^* = F'[p]^*$  as in Corollary 12.

Similarly, if only the real part of the data can be observed, analogous formulas hold true with  $R$  replaced by the real-part operator  $\Re : L^2_{\mathbb{C}}(I, r^2 \sin) \rightarrow L^2_{\mathbb{R}}(I, r^2 \sin)$ , of which the Hilbert space adjoint is the canonical embedding of  $L^2_{\mathbb{R}}(I, r^2 \sin)$  into  $L^2_{\mathbb{C}}(I, r^2 \sin)$ .

## 5 Tangential cone condition

As discussed in Section 4, the inverse problem under consideration is ill-posed, necessitating the use of regularization to achieve stable reconstruction of the target coefficients. Iterative gradient-based regularization methods, such as Landweber iteration, Newton-type schemes, and their variants, fundamentally rely on three core elements: the well-posedness of the forward operator  $F$  (Section 3), adjoint of the linearized operator (Section 4.2), and guarantees of convergence. This final requirement is typically ensured by making specific structural assumptions about  $F$ , particularly regarding its nonlinearity and the uniform boundedness of its derivative; these issues are the main focus of this section.

To address this, we consider the tangential cone condition (TCC), a celebrated criterion first introduced in [16] that ensures local convergence of iterative regularization algorithms. Intuitively, if the forward map  $F$  is excessively nonlinear, there is no general guarantee that gradient descent steps will remain within the vicinity of the true solution. The tangential cone condition offers a quantitative tool for assessing the nonlinearity of  $F$ , especially in the context of compact operators, thereby paving the way for the successful application of iterative regularization methods. Notably,

satisfaction of this condition also implies uniqueness of the minimum-norm solution, and, combined with the null space condition, ensures that the iterative reconstruction sequence converges to this solution [22].

For a general model  $F : X \ni p \mapsto y \in Y$ , TCC is stated in the following (strong) form, that is the inequality

$$\|F(p) - F(\tilde{p}) - F'(p)(p - \tilde{p})\|_Y \leq C_{tc} \|p - \tilde{p}\|_X \|F(p) - F(\tilde{p})\|_Y \quad \text{for all } p, \tilde{p} \in B_R^X(p^\dagger)$$

holds for some constant  $C_{tc} > 0$  and radius  $R > 0$  of the ball around a ground truth  $p^\dagger \in \mathcal{D}(F)$ ; see also [25] for the weak forms. In our setting, TCC reads as

$$\begin{aligned} \|F(\gamma, \Omega) - F(\tilde{\gamma}, \tilde{\Omega}) - F'[\gamma, \Omega]((\gamma, \Omega) - (\tilde{\gamma}, \tilde{\Omega}))\|_Y & \quad (40) \\ & \leq C_{tc} \|(\gamma, \Omega) - (\tilde{\gamma}, \tilde{\Omega})\|_{\mathbb{R} \times X} \|F(\gamma, \Omega) - F(\tilde{\gamma}, \tilde{\Omega})\|_Y \\ & \quad \text{for all } (\gamma, \Omega), (\tilde{\gamma}, \tilde{\Omega}) \in B_R^{\mathbb{R} \times X}(\gamma^\dagger, \beta^\dagger). \end{aligned}$$

It is worth noting that, in addition to the TCC, several other conditions can be employed to characterize the structure of the forward map and provide convergence guarantees. Notable examples include range-invariance [24], convexity, and the Polyak-Lojasiewicz condition [31].

Although the tangential cone condition is a powerful tool, it can be challenging to verify in practice; for a general verification strategy with full data, we refer the reader to [23]. Contributions in this area span a wide range of applications, including elliptic inverse problems [18], elastography [21, 20], electrical impedance tomography [26], full waveform inversion [10], and more recently, neural network-based inverse problems [35, 1].

In this work, we contribute to the literature by establishing the tangential cone condition for full measurements, introducing a lifted regularity strategy developed in Section 3.4 to account for realistic measured data in  $L^2$ . Furthermore, we extend our verification to the setting of restricted measurements.

## 5.1 Full measurement

**Lemma 14** (Uniform boundedness). *Given the setting in Proposition 8. The operators  $\mathbf{B}_m(\gamma^\dagger, \Omega^\dagger)^{-1}$  are bounded from  $H_\diamond^{-4}(r\mathbb{S}^2; m)$  to  $L_\diamond^2(r\mathbb{S}^2; m)$  for all  $(\gamma^\dagger, \Omega^\dagger) \in \mathcal{D}(S) \cap (\mathbb{R}^+ \times H^2(r\mathbb{S}^2; m = 0))$ . Moreover, they are locally uniformly bounded in the sense that there exists  $\bar{R}(\gamma^\dagger, \Omega^\dagger) > 0$  such that*

$$N^{\gamma^\dagger, \Omega^\dagger}(R) := \sup \left\{ \|\mathbf{B}_m(\gamma, \Omega)^{-1}\|_{H^{-4} \rightarrow L^2} : (\gamma, \Omega) \in B_R^{\mathbb{R} \times X}(\gamma^\dagger, \Omega^\dagger) \right\}$$

is finite for all  $R \leq \bar{R}(\gamma^\dagger, \Omega^\dagger)$ , and  $B_R^{\mathbb{R} \times X}(\gamma^\dagger, \Omega^\dagger) \subset \mathcal{D}(S)$ .

*Proof.* Boundedness follows from the lifted regularity result in Proposition 8 and that  $\mathbf{B}_m(\gamma^\dagger, \Omega^\dagger) : L_\diamond^2(r\mathbb{S}^2; m) \rightarrow H_\diamond^{-4}(r\mathbb{S}^2; m)$  is the Banach adjoint of  $\mathbf{B}_m(\gamma^\dagger, \Omega^\dagger)^* : H_\diamond^4(r\mathbb{S}^2; m) \rightarrow L_\diamond^2(r\mathbb{S}^2; m)$ . The local uniformity of norm bounds can be seen from the fact that the norms of  $\gamma, \Omega$  appear in an affine linear manner in all upper bounds in the proof of Proposition 8.  $\square$

**Theorem 15** (TCC – full measurement). *Given the setting in Proposition 8. For  $m \neq 0$ , the forward operator  $F$  with full measurements satisfies the TCC (40).*

*Proof.* Recall  $F = S$  for the full measurements. For any  $p^\dagger = (\gamma^\dagger, \Omega^\dagger) \in \mathcal{D}(S)$ , we have to show that there exists  $R, C_{\text{tc}} > 0$  such that

$$\|S(p+h) - S(p) - S'[p]h\|_{L^2} \leq C_{\text{tc}} \|h\|_{\mathbb{R} \times H^2} \|S(p) - S(p+h)\|_{L^2}$$

with  $h := \tilde{p} - p$ , for all  $p, \tilde{p} \in B_R^{\mathbb{R} \times X}(\gamma^\dagger, \beta^\dagger)$ . Using the identity  $\mathbf{B}_m(p+h) - \mathbf{B}_m(p) = \mathbf{B}'_m(h)$  and twice the identity  $T^{-1} - S^{-1} = T^{-1}(S - T)S^{-1}$  for invertible operators  $S$  and  $T$ , we obtain

$$\begin{aligned} S(p+h) - S(p) - S'[p]h &= \mathbf{B}_m(p+h)^{-1}f - \mathbf{B}_m(p)^{-1}f + \mathbf{B}_m(p)^{-1}\mathbf{B}'_m(h)S(p) \\ &= [-\mathbf{B}_m(p+h)^{-1} + \mathbf{B}_m(p)^{-1}]\mathbf{B}'_m(h)S(p) \\ &= \mathbf{B}_m(p)^{-1}\mathbf{B}'_m(h)\mathbf{B}_m(p+h)^{-1}\mathbf{B}'_m(h)\mathbf{B}_m(p)^{-1}f \\ &= -\mathbf{B}_m(p)^{-1}\mathbf{B}'_m(h)(S(p+h) - S(p)). \end{aligned}$$

Therefore, it suffices to show that  $\|\mathbf{B}_m(p)^{-1}\mathbf{B}'_m(h)\|_{L^2 \rightarrow L^2} \leq C_{\text{tc}} \|h\|_{\mathbb{R} \times H^2}$ .

We first estimate  $\|\mathbf{B}'_m(h)\|_{L^2 \rightarrow H^{-4}}$ . Let  $h =: (\delta\gamma, \delta\Omega)$ , for  $w \in L^2(r\mathbb{S}^2; m)$  and  $\varphi \in H_\diamond^4(r\mathbb{S}^2; m)$ , we obtain the following bound on the inner product:

$$\begin{aligned} \langle \mathbf{B}'_m(h)w, \varphi \rangle &= \langle \delta\gamma w, \Delta_m^2 \varphi \rangle - \langle im(\delta\Omega)w, \Delta_m \varphi \rangle + \langle imw, \alpha_{\delta\Omega} \varphi \rangle \\ &\leq |\delta\gamma| \|w\|_{L^2} \|\varphi\|_{H^4} + |m| \|\delta\Omega\|_{L^\infty} \|w\|_{L^2} \|\varphi\|_{H^2} + C_\alpha |m| \|\delta\Omega\|_{H^2} \|w\|_{L^2} \|\varphi\|_{H^2} \\ &\leq C_{\text{emb}} \|h\|_{\mathbb{R} \times \tilde{X}} \|w\|_{L^2} \|\varphi\|_{H^4} \end{aligned}$$

where  $C_{\text{emb}} := \sqrt{2} \max\{1, |m|C_{H^4 \rightarrow H^2}(C_{H^2 \rightarrow L^\infty} + C_\alpha)\}$  with  $C_\alpha$  as in (29). This shows that

$$\|\mathbf{B}'_m(h)\|_{L^2 \rightarrow H^{-4}} \leq C_{\text{emb}} \|h\|_{\mathbb{R} \times \tilde{X}}.$$

Then, together with the locally uniform boundedness in Lemma 14, we achieve

$$\begin{aligned} \|\mathbf{B}_m(p)^{-1}\mathbf{B}'_m(h)\|_{L^2 \rightarrow L^2} &\leq \|\mathbf{B}_m(p)^{-1}\|_{H^{-4} \rightarrow L^2} \|\mathbf{B}'_m(h)\|_{L^2 \rightarrow H^{-4}} \\ &\leq N^{\gamma^\dagger, \Omega^\dagger}(R) C_{\text{emb}} \|h\|_{\mathbb{R} \times H^2}. \end{aligned} \tag{41}$$

In this step, we observe the importance of the lifted regularity laid out in Section 3.4, which is the key to Lemma 14. This proves the TCC (40) in  $B_R^X(p^\dagger)$ .  $\square$

## 5.2 Partial measurement including Cauchy data

We now turn to the case of restricted measurements, where observations are limited to  $I' = (\epsilon, \pi - \epsilon)$  as described in Section 2.3. As a simplification, we additionally assume that Cauchy data at the boundary of  $I'$  can be measured exactly. We follow the analysis for the full Sun, while specifically leveraging the well-posedness and regularity results for the restricted domain established in Section 3.5, Proposition 9.

**Theorem 16** (TCC – partial measurement). *Consider the setting in Proposition 9, (ii). If one imposes the constraint*

$$\Psi|_{\partial I'} = \Psi^\dagger|_{\partial I'} \quad \text{and} \quad \Psi'|_{\partial I'} = (\Psi^\dagger)'|_{\partial I'}, \quad (42)$$

where  $\Psi^\dagger$  is the exact state, then for  $m \neq 0$ , the forward operator  $F$  with partial measurements satisfies the TCC (40).

*Proof.* The proof is almost identical to that of Theorem 15. Note that  $S(p+h) - S(p)$  and  $S'(p)$  both satisfy homogeneous Cauchy boundary conditions on  $\partial I'$ . This allows us to carry out partial integration as before and prove that

$$\begin{aligned} \|\mathbf{B}_m(p)^{-1}\mathbf{B}'_m(h)\|_{L^2(I') \rightarrow L^2(I')} &\leq \|\mathbf{B}_m(p)^{-1}\|_{H^{-4}(I') \rightarrow L^2(I')} \|\mathbf{B}'_m(h)\|_{L^2(I') \rightarrow H^{-4}(I')} \\ &\leq N^{\gamma^\dagger, \Omega^\dagger}(R) C_{\text{emb}} \|h\|_{\mathbb{R} \times H^2(I'; m=0)} \\ &\leq N^{\gamma^\dagger, \Omega^\dagger}(R) C_{\text{emb}} \|h\|_{\mathbb{R} \times H^2(r\mathbb{S}^2; m=0)} \end{aligned}$$

for any  $p, p+h$  in the ball  $B_R^X(p^\dagger)$ .  $\square$

It is worth remarking that the constraint assumption in (42), which requires knowledge of the exact solution on the boundary, is an essential component to the proof of Theorem 16; relaxing this condition poses an interesting question for future research.

## 6 Numerical experiments

We implemented the accelerated Nesterov-Landweber method to simultaneously reconstruct the scalar viscosity and latitudinal differential rotation parameters,  $(\gamma, \Omega)$ . A convergence analysis of this method has been carried out in [19, 29] under the tangential cone condition, which we have been verified for our problem in Section 5. The Nesterov-Landweber iteration proceeds as follows: initiate  $p_{-1} = p_0 := (\gamma_{\text{int}}, \Omega_{\text{int}})$ , then run

$$\begin{aligned} z_k &= p_k + \frac{k-1}{k+\alpha-1} (p_k - p_{k-1}) \quad \alpha = 3 \\ p_{k+1} &= z_k - \mu_k F'(z_k)^* \left( F(z_k) - y^\delta \right) \quad k \leq K(y^\delta, \delta). \end{aligned} \quad (43)$$

Here, the forward map  $F$  corresponds to the wave equation at single frequency  $\omega$  and longitudinal wavenumber  $m$ . We allow for different observation strategies: full data, leaked data, and real part measurements. The Hilbert space adjoints  $F'(z_k)^*$  are derived in Section 4.2. The inversion takes place in the following function spaces:  $\gamma \in \mathbb{R}$ ,  $\Omega \in H^2(r\mathbb{S}^2, m=0)$ , thus ensuring convergence of the reconstruction.

The numerical wave solution uses a fourth-order finite difference scheme [39] on a uniform grid of 100 points spanning the latitude range  $(0, \pi)$ . To generate ground truths while avoiding inverse crimes, we explicitly choose analytic  $\Psi_{m, \gamma}$  and  $\Omega$  with Dirichlet boundary, then explicitly obtain the corresponding source  $f$ . The discrete

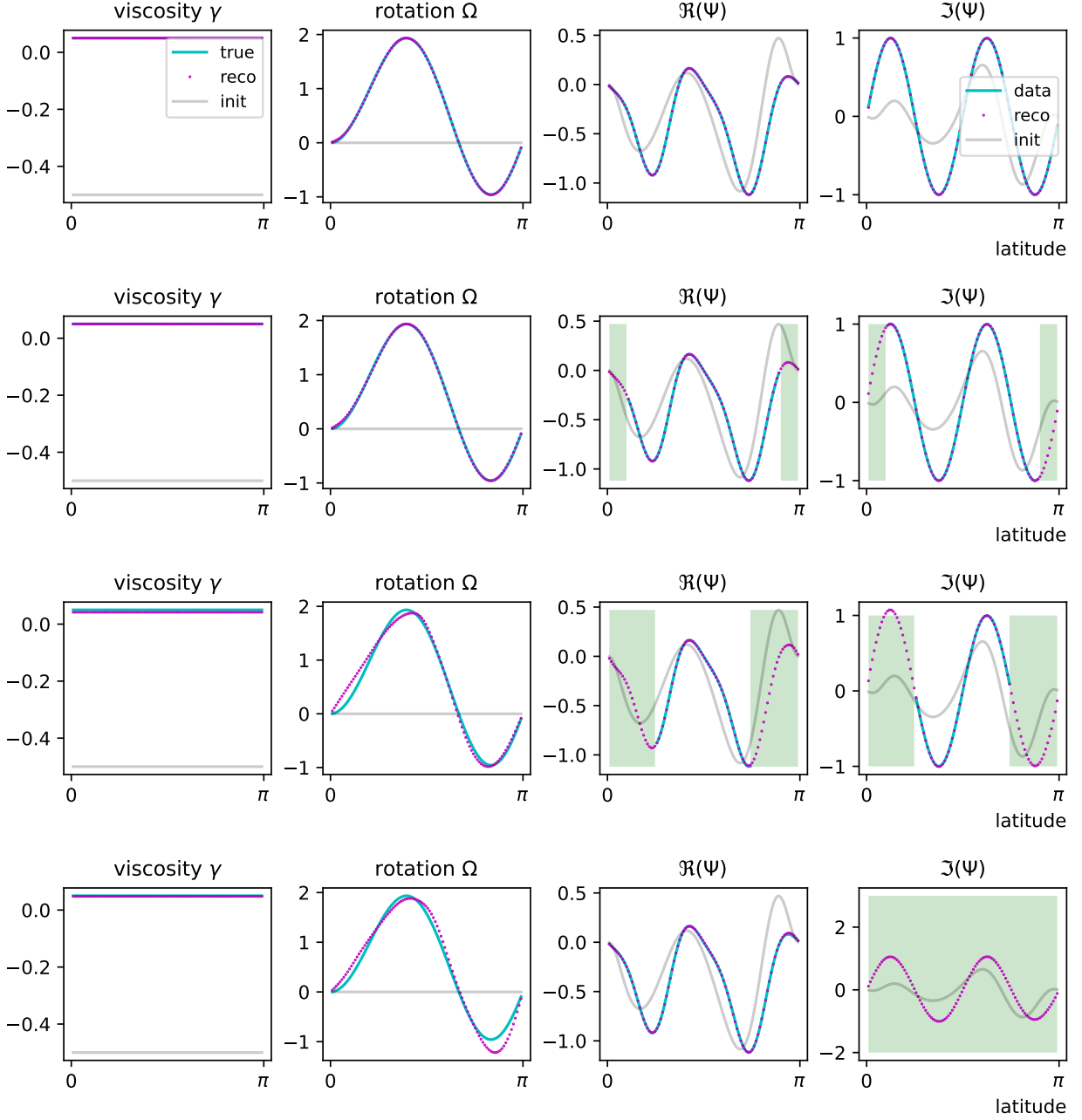


Figure 1: Clean data. Top to bottom: full and leaked data (filled area) at different levels.

measurement  $\underline{y}^\delta$  is corrupted by independent additive complex Gaussian noise with variance  $\sigma^2$  on 100 equidistant measurement points and  $\sigma$  chosen to have relative noise levels  $\|\underline{y}^\delta - \underline{y}\|_2 / \|\underline{y}\|_2 \in \{0.01, 0.05, 0.2\}$ .

We initialize the algorithm with  $\gamma_{\text{int}} = -3\gamma_{\text{true}}$  and  $\Omega_{\text{int}} = 0$ , corresponding to no prior knowledge of the ground truth, and iterate with a step size  $\mu_k$  determined by backtracking line search. The stopping criterion is the first instance when the

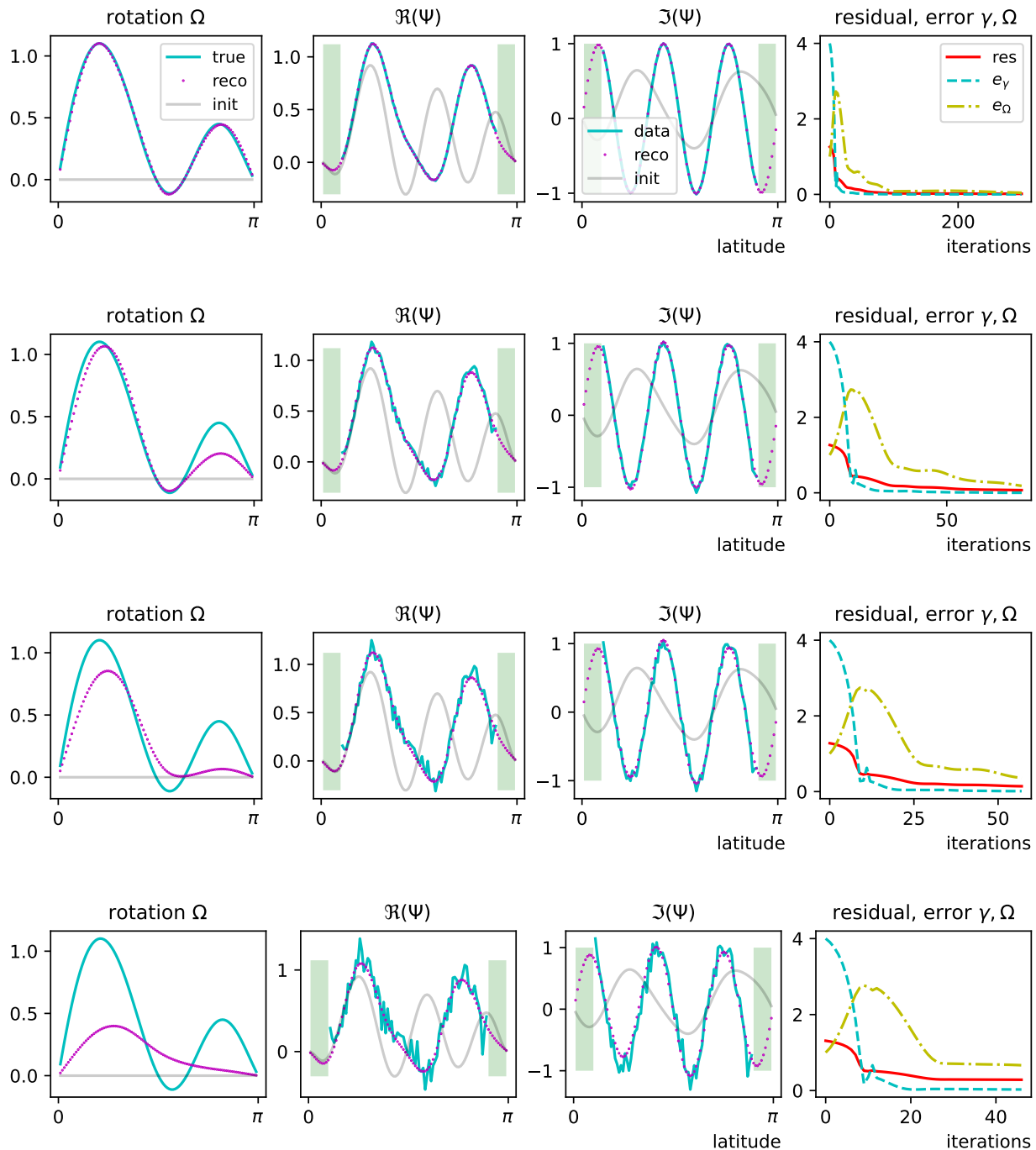


Figure 2: Leaked data. Top to bottom: 1%, 5%, 10%, 20% relative noise level.

residual falls below the threshold  $\tau\delta$  (with  $\tau = 1.1$ ), which in practice yields better results than choosing  $\tau > 2$  [19]. The algorithm typically completes 200 iterations within one second on an i7-1255U CPU (4.70 GHz).

**Full data.** Figure 1, row 1 shows the simultaneous recovery of  $(\gamma, \Omega)$  from full, noise-free measurements of the state  $\Psi$  at  $(\omega, m) = (3, 3)$ . Despite of an initial guess far from the ground truth, the reconstruction closely approximates the exact parameters. The reconstructed wave field also matches the true state in both real and imaginary parts.

**Leaked data at poles.** Figure 1, rows 2–3 present the practical case where no data are available near the poles. In our numerical experiments, we did not impose additional Cauchy boundary data in Theorem 16, and simply computed the adjoint as described in Remark 13. With 20% of the data leaked, the reconstruction quality remains nearly as high as with full data. For 50% data loss, the recovery of  $\Omega$  moderately deteriorates. Nonetheless, the algorithm exhibits robust performance, consistent with our convergence results in Section 5.2.

**Real part measurement.** Figure 1, row 4 considers the scenario where only the real part of  $\Psi$  is measured. Compared to row 3 (which also has 50% data leakage, but full complex data), the absence of the imaginary component further impairs the reconstruction, most notably in missing the secondary peak of the differential rotation.

**Noisy data.** Finally, Figure 2 reports the results with both data leakage and measurement noise, for  $(\omega, m) = (1, 2)$ . At 1% noise, the recovered parameters remain very close to the truth, as evidenced by small relative errors  $(\|p - p_{\text{true}}\|_{L^2} / \|p_{\text{true}}\|_{L^2})$ . At 5% noise, reconstruction quality is slightly reduced, while at 20% noise, the outcome degrades significantly.

## 7 Conclusions and Outlook

In this paper, we examined the modeling, as well as the associated forward and inverse problems, for inertial waves on the surface of the Sun. Formulating the dynamics in terms of a stream function leads to a fourth-order elliptic differential equation on the sphere. We rigorously proved well-posedness of this equation, including explicit smallness conditions for uniqueness, as well as conditions for non-uniqueness via analytic Fredholm theory, both in agreement with empirical findings in helioseismology. Our studies represent the starting point for further theoretical and numerical studies of resonances and inertial modes, as well as the associated inverse problems.

For the inverse problem of simultaneous identification of differential rotation and viscosity, we established convergence guarantees for the iterative reconstruction process via the tangential cone condition. For the case of partial observations, this required the additional assumption of exact observations of Cauchy boundary data. It is natural to ask whether this assumption can be relaxed, e.g., by including the Cauchy data in the range of the operator. We point out that at least for a finite number of  $m$  and  $\omega$ , uniqueness of rotation at the unobserved latitudes seems unrealistic by dimensionality arguments.

Next steps include the incorporation of physical effects such as radial motion, pressure, and gravity [14] into the model and inversions with solar-like parameters, including realistic convection noise [32], as well as real observational data from the Helioseismic and Magnetic Imager. Another promising avenue involves leveraging data-driven model discovery techniques [1, 30] to refine existing theoretical models by learning hidden laws.

## A Differential geometry and function spaces on spheres

Let  $\mathbb{S}^2 := \{\mathbf{r} \in \mathbb{R}^3 : |\mathbf{r}| = 1\}$  denote the unit sphere in  $\mathbb{R}^3$  and  $r\mathbb{S}^2 = \{r\mathbf{r} : \mathbf{r} \in \mathbb{S}^2\} = \{\mathbf{r} \in \mathbb{R}^3 : |\mathbf{r}| = r\}$  the sphere of radius  $r > 0$ . In this appendix, we recall some differential operators on  $r\mathbb{S}^2$  and their properties as well as function spaces on  $r\mathbb{S}^2$ , which are used throughout this paper.

**Spherical coordinates.** We use  $\mathbf{r}(r, \theta, \phi) := (r \sin \theta \cos \phi, r \sin \theta \sin \phi, r \cos \theta)$  as definition of spherical coordinates with radial distance  $r > 0$ , polar angle  $\theta \in (0, \pi)$  and azimuthal angle  $\phi \in (0, 2\pi)$ . In our notation, we do not distinguish between a function  $f : \mathbb{R}^3 \rightarrow \mathbb{R}$  and its counterpart  $f \circ \mathbf{r} : (0, \infty) \times (0, \pi) \times (0, 2\pi) \rightarrow \mathbb{R}$  in spherical coordinates. Note that the vectors  $\{\mathbf{e}_r(\mathbf{r}), \mathbf{e}_\theta(\mathbf{r}), \mathbf{e}_\phi(\mathbf{r})\}$  defined by  $\mathbf{e}_r(\mathbf{r}) := \frac{\partial \mathbf{r}}{\partial r} / \left| \frac{\partial \mathbf{r}}{\partial r} \right|$  and similarly for  $\mathbf{e}_\theta$  and  $\mathbf{e}_\phi$  form a local orthonormal basis for all  $\mathbf{r}$ .

**Differential operators on the sphere.** A vector-valued function  $\mathbf{f} : r\mathbb{S}^2 \rightarrow \mathbb{R}^3$  is called *tangential* if  $\mathbf{f}(\mathbf{r}) \cdot \mathbf{e}_r(\mathbf{r}) = 0$  for all  $\mathbf{r}$ . For a tangential vector field  $\mathbf{f}$  and a scalar  $f$  on  $r\mathbb{S}^2$ , consider any smooth extensions  $\tilde{\mathbf{f}}$  and  $\tilde{f}$  to a neighborhood of  $r\mathbb{S}^2$  in  $\mathbb{R}^3$ . Then it is possible to define the surface (or horizontal) gradient  $\mathbf{grad}_h f$ , the surface divergence  $\text{div}_h \mathbf{f}$ , and the scalar and vectorial surface curl  $\text{curl}_h \mathbf{f}$  and  $\mathbf{curl}_h f$  such that

$$\begin{aligned} \mathbf{grad}_h f &= (\mathbf{grad} \tilde{f} - \frac{\partial \tilde{f}}{\partial r} \mathbf{e}_r)|_{r\mathbb{S}^2}, & \text{div}_h \mathbf{f} &= \text{div} \tilde{\mathbf{f}}|_{r\mathbb{S}^2}, \\ \mathbf{curl}_h f &= \text{curl}(\tilde{f} \mathbf{e}_r)|_{r\mathbb{S}^2}, & \text{curl}_h \mathbf{f} &= (\text{curl} \tilde{\mathbf{f}} \cdot \mathbf{e}_r)|_{r\mathbb{S}^2} \end{aligned} \quad (44)$$

independent of the choices of  $\tilde{f}$  and  $\tilde{\mathbf{f}}$  (see [28, p. 72–73]). Here  $\text{div}_h \mathbf{f}$  and  $\text{curl}_h \mathbf{f}$  are scalar functions, while  $\mathbf{grad}_h f$  and  $\mathbf{curl}_h f$  are tangential vector fields on  $r\mathbb{S}^2$ . In spherical coordinates, writing  $\mathbf{f} = f_\theta \mathbf{e}_\theta + f_\phi \mathbf{e}_\phi$  with  $f_\theta := \mathbf{f} \cdot \mathbf{e}_\theta$  and  $f_\phi := \mathbf{f} \cdot \mathbf{e}_\phi$ , we have

$$\begin{aligned} \mathbf{grad}_h f &= \frac{1}{r} \frac{\partial f}{\partial \theta} \mathbf{e}_\theta + \frac{1}{r \sin \theta} \frac{\partial f}{\partial \phi} \mathbf{e}_\phi, & \text{div}_h \mathbf{f} &= \frac{1}{r \sin \theta} \left( \frac{\partial}{\partial \theta} (f_\theta \sin \theta) + \frac{\partial f_\phi}{\partial \phi} \right), \\ \mathbf{curl}_h f &= \frac{1}{r \sin \theta} \frac{\partial f}{\partial \phi} \mathbf{e}_\theta - \frac{1}{r} \frac{\partial f}{\partial \theta} \mathbf{e}_\phi, & \text{curl}_h \mathbf{f} &= \frac{1}{r \sin \theta} \left( \frac{\partial}{\partial \theta} (f_\phi \sin \theta) - \frac{\partial f_\theta}{\partial \phi} \right). \end{aligned} \quad (45)$$

These differential operators satisfy the identities ([28, Thm. 2.5.19]):

$$\begin{aligned} \operatorname{curl}_h \mathbf{grad}_h &= 0, & \operatorname{div}_h \mathbf{curl}_h &= 0, \\ \int_{r\mathbb{S}^2} \mathbf{grad}_h f \cdot \mathbf{f} \, ds &= - \int_{r\mathbb{S}^2} f \operatorname{div}_h \mathbf{f} \, ds, & \int_{r\mathbb{S}^2} \mathbf{curl}_h f \cdot \mathbf{f} \, ds &= \int_{r\mathbb{S}^2} f \operatorname{curl}_h \mathbf{f} \, ds. \end{aligned} \quad (46)$$

The Laplace-Beltrami operator on  $r\mathbb{S}^2$  is given by

$$\Delta_h f = \operatorname{div}_h \mathbf{grad}_h f = - \operatorname{curl}_h \mathbf{curl}_h f, \quad (47)$$

and the vector Laplacian or Hodge operator acting on tangential vector fields  $\mathbf{f}$  is defined as

$$\Delta_h \mathbf{f} = \mathbf{grad}_h \operatorname{div}_h \mathbf{f} - \mathbf{curl}_h \operatorname{curl}_h \mathbf{f}. \quad (48)$$

We also need a decomposition of  $L^2_{\tan}(r\mathbb{S}^2) := \{\mathbf{f} \in L^2(r\mathbb{S}^2, \mathbb{R}^3) : \mathbf{f} \cdot \mathbf{e}_r \equiv 0\}$  into two orthogonal subspaces. Since  $r\mathbb{S}^2$  is simply connected, there exist for each tangential vector field  $\mathbf{f} \in L^2_{\tan}(r\mathbb{S}^2)$  two functions  $\varphi, \psi \in H^1(r\mathbb{S}^2)$  such that

$$\mathbf{f} = \mathbf{grad}_h \varphi + \mathbf{curl}_h \psi, \quad (49)$$

and  $\langle \mathbf{grad}_h \varphi, \mathbf{curl}_h \psi \rangle_{L^2} = 0$  (see [28, Eq. (5.6.24)]).

**Function spaces.** We define Sobolev spaces  $H^s(r\mathbb{S}^2)$  as Hilbert scale generated by the operator  $(I - \Delta_h)^{1/2}$ :

$$H^s(r\mathbb{S}^2) := \operatorname{dom}((I - \Delta_h)^{s/2}) \quad \text{with} \quad \|f\|_{H^s} := \|(I - \Delta_h)^{s/2} f\|_{L^2}$$

for  $s \geq 0$ . It is straightforward that these are Hilbert spaces, and that  $H^0(r\mathbb{S}^2) := L^2(r\mathbb{S}^2)$ . Moreover, we set  $H^{-s}(r\mathbb{S}^2) := H^s(r\mathbb{S}^2)^*$  with the natural norm. We further introduce subspaces of functions with mean 0 by

$$L^2_{\diamond}(r\mathbb{S}^2) := \{f \in L^2(r\mathbb{S}^2) : \langle f, 1 \rangle = 0\}, \quad H^s_{\diamond}(r\mathbb{S}^2) := \{f \in H^s : \langle f, 1 \rangle = 0\} \quad (50)$$

for  $s \in \mathbb{R}$ . These spaces are also complete with the same norms, but we will later define a slightly more convenient equivalent norm on  $H^s_{\diamond}(r\mathbb{S}^2)$ .

The following embeddings hold true (see [36, Propositions 3.2-3.3], [17, Theorem 3.5]):

$$H^s(r\mathbb{S}^2) \hookrightarrow H^k(r\mathbb{S}^2) \quad \text{compact for } s > k \quad (51a)$$

$$H^s(r\mathbb{S}^2) \hookrightarrow L^p(r\mathbb{S}^2) \quad \text{continuous for } s \geq \max(0, 1 - \frac{2}{p}) \text{ and } p \in [1, \infty) \quad (51b)$$

$$H^s(r\mathbb{S}^2) \hookrightarrow C^k(r\mathbb{S}^2) \quad \text{compact for } s > k + 1 \text{ with } k \geq 0. \quad (51c)$$

**Azimuthal Fourier transform.** Writing a function  $f \in L^2(r\mathbb{S}^2)$  in spherical coordinates  $f = f(\theta, \phi)$ , we can perform a Fourier transform in  $\phi$  to expand  $f$  into a Fourier series

$$f(\theta, \phi) = \frac{1}{\sqrt{2\pi}} \sum_{m=-\infty}^m \hat{f}_m(\theta) e^{im\phi}. \quad (52)$$

Let us define  $e_m(\phi) := (2\pi)^{-1/2}e^{im\phi}$  and  $(\hat{f}_m \otimes e_m)(\theta, \phi) := \hat{f}_m(\theta)e^{im\phi}$ . Since  $\hat{f}_m \otimes e_m \perp \hat{f}_n \otimes e_n$  in  $L^2(r\mathbb{S}^2)$  and in  $L_\diamond^2(r\mathbb{S}^2)$  for  $m \neq n$ , the expression (52) induces orthogonal decompositions

$$L^2(r\mathbb{S}^2) = \bigoplus_{m=-\infty}^{\infty} L^2(r\mathbb{S}^2; m), \quad L_\diamond^2(r\mathbb{S}^2) = \bigoplus_{m=-\infty}^{\infty} L_\diamond^2(r\mathbb{S}^2; m) \quad (53)$$

with  $\hat{f}_m \otimes e_m \in L^2(r\mathbb{S}^2; m)$ . As the spherical harmonics  $\{Y_{lm} : l \in \mathbb{N}_0, m \in \mathbb{Z}, |m| \leq l\}$  form a complete orthonormal basis of  $L^2(r\mathbb{S}^2)$  and  $Y_{lm} \in L^2(r\mathbb{S}^2; m)$ , we have

$$\begin{aligned} L^2(r\mathbb{S}^2; m) &= L_\diamond^2(r\mathbb{S}^2; m) = \overline{\text{span}\{Y_{lm} : l \geq |m|\}}^{L^2}, \quad m \in \mathbb{Z} \setminus \{0\}, \\ L^2(r\mathbb{S}^2; 0) &= \overline{\text{span}\{Y_{l0} : l \in \mathbb{Z}\}}^{L^2}, \quad L_\diamond^2(r\mathbb{S}^2; 0) = \overline{\text{span}\{Y_{l0} : l \in \mathbb{Z} \setminus \{0\}\}}^{L^2}, \end{aligned}$$

where span denotes the set of *finite* linear combinations. The Laplace-Beltrami operator is diagonal with respect to the decompositions (53). More precisely, it follows from (44) and (47) that

$$\Delta_{\text{h}} f = \sum_{m=-\infty}^{\infty} (\hat{\Delta}_m \hat{f}_m) \otimes e_m \quad \text{with} \quad \hat{\Delta}_m := \frac{1}{r^2 \sin \theta} \frac{d}{d\theta} \left( \sin \theta \frac{d}{d\theta} \right) - \frac{m^2}{r^2 \sin^2 \theta}. \quad (54)$$

Let us also define  $\Delta_m(\hat{f}_m \otimes e_m) := (\hat{\Delta}_m \hat{f}_m) \otimes e_m$ . We obtain  $H^s$ -orthogonal decompositions

$$H^s(r\mathbb{S}^2) = \bigoplus_{m \in \mathbb{Z}} H^s(r\mathbb{S}^2; m) \quad \text{and} \quad H_\diamond^s(r\mathbb{S}^2) = \bigoplus_{m \in \mathbb{Z}} H_\diamond^s(r\mathbb{S}^2; m) \quad (55)$$

for any  $s \in \mathbb{R}$ , where  $H^s(r\mathbb{S}^2; m)$  and  $H_\diamond^s(r\mathbb{S}^2; m)$  are the closures of  $\text{span}\{Y_{lm} : l \geq |m|\}$  in  $H^s(r\mathbb{S}^2)$  and  $H_\diamond^s(r\mathbb{S}^2)$ , respectively. Again,  $H^s(r\mathbb{S}^2; m) = H_\diamond^s(r\mathbb{S}^2; m)$  for  $m \in \mathbb{Z} \setminus \{0\}$  and  $H^s(r\mathbb{S}^2; 0) = H_\diamond^s(r\mathbb{S}^2; 0) \oplus \text{span}\{1\}$ . As  $-\Delta_{\text{h}} Y_{lm}(\cdot/r) = \frac{l(l+1)}{r^2} Y_{lm}(\cdot/r)$ , and  $Y_{00}(\cdot/r) \notin L_\diamond^2(r\mathbb{S}^2)$ , it follows that  $\langle -\Delta_{\text{h}} f, f \rangle \geq 2/r^2 \|f\|_{L^2}^2$  for all  $f \in L_\diamond^2(r\mathbb{S}^2)$ . Consequently,

$$\|f\|_{H_\diamond^s} := \|(-\Delta_{\text{h}})^{s/2} f\|_{L^2}, \quad s \geq 0$$

defines a norm on  $H_\diamond^s(r\mathbb{S}^2)$  which is equivalent to the  $\|\cdot\|_{H^s}$ -norm. We will consider this as the standard norm on  $H_\diamond^s(r\mathbb{S}^2)$  as it has the convenient properties

$$\begin{aligned} \|f\|_{H_\diamond^2} &= \|\Delta_{\text{h}} f\|_{L^2} \quad \text{and} \\ \|f\|_{H_\diamond^1}^2 &= \langle -\Delta_{\text{h}} f, f \rangle = \langle -\text{div}_{\text{h}} \mathbf{grad}_{\text{h}} f, f \rangle = \|\mathbf{grad}_{\text{h}} f\|_{L^2}^2. \end{aligned} \quad (56)$$

Defining  $H_\diamond^{-s}(r\mathbb{S}^2) := H_\diamond^s(r\mathbb{S}^2)'$  for  $s > 0$  we have that

$$\Delta_{\text{h}} : H_\diamond^t(r\mathbb{S}^2) \rightarrow H_\diamond^{t-2}(r\mathbb{S}^2) \quad \text{is an isometric isomorphism for all } t \in \mathbb{R}. \quad (57)$$

Defining  $L^p(r\mathbb{S}^2; m)$  as the closure of  $\text{span}\{Y_{lm} : l \geq |m|\}$  in  $L^p(r\mathbb{S}^2)$ , the embeddings (51) implies the embeddings in the decomposed spaces

$$H^s(r\mathbb{S}^2; m) \hookrightarrow H^k(r\mathbb{S}^2; m) \quad \text{compact for } s > k \quad (58a)$$

$$H^s(r\mathbb{S}^2; m) \hookrightarrow L^p(r\mathbb{S}^2; m) \quad \text{continuous for } s \geq \max(0, 1 - \frac{2}{p}), p \in [1, \infty). \quad (58b)$$

## B Boundary conditions

The following lemma describes homogeneous boundary conditions satisfied by the  $\theta$ -dependent factors of separated smooth solutions:

**Lemma 17.** *Let  $m \in \mathbb{Z}$  and  $k \in \mathbb{N}_0 = \{0, 1, 2, \dots\}$ . A function of the form  $u(\theta, \phi) = u_m(\theta) \exp(im\phi)$  in spherical coordinates belongs to  $C^k(r\mathbb{S}^2)$  if and only if the following three conditions are satisfied:*

- (i)  $u_m \in C^k([0, \pi])$ ,
- (ii)  $u_m^{(j)}(\theta) = 0$  for  $\theta \in \{0, \pi\}$  and all  $j \in \mathbb{N}_0$  with  $j \leq k$  and  $(-1)^{|m|+j} = -1$ ,
- (iii)  $u_m^{(j)}(\theta) = 0$  for  $\theta \in \{0, \pi\}$  and all  $j \in \mathbb{N}_0$  with  $j < m$ .

*Proof.* It is clear that  $u_m \in C^k([0, \pi])$  is equivalent to  $u \in C^k(r\mathbb{S}^2 \setminus \{P_+, P_-\})$  with the poles  $P_{\pm} := (0, 0, \pm 1)$ . Moreover, as  $u_m(\theta) = u(\theta, 0)$ , we have  $u_m \in C^k([0, \pi])$  if  $u \in C^k(r\mathbb{S}^2)$ .

To study regularity at the pole  $P_+$ , consider the smooth map  $M : D := \{(x, y) \in \mathbb{R}^2 : x^2 + y^2 \leq r^2/2\} \rightarrow r\mathbb{S}^2$  of  $r\mathbb{S}^2$  defined by  $M(x, y) := \sqrt{r^2 - x^2 - y^2}$ . By definition,  $u$  is  $k$ -times differentiable at  $P_+$  if and only if  $u \circ M$  is  $k$  times differentiable at 0. And this is the case if and only if there exists a polynomial  $p(x, y) = \sum_{j=0}^k \sum_{n=0}^j c_{j,n} x^n y^{j-n}$  of degree  $\leq k$  such that

$$|(u \circ M - p)(x, y)| = o\left(\sqrt{x^2 + y^2}^k\right) \quad \text{as } (x, y) \rightarrow 0. \quad (59)$$

Writing  $x = \frac{\rho}{2}(e^{i\phi} + e^{-i\phi})$  and  $y = \frac{i\rho}{2}(e^{i\phi} - e^{-i\phi})$  in polar coordinates and using binomial expansions, we obtain

$$\sum_{n=0}^j c_{j,n} x^n y^{j-n} = \rho^j \sum_{l=0}^j d_{j,l} e^{i(j-2l)\phi}$$

for some coefficients  $d_{j,l} \in \mathbb{C}$ . As  $(u \circ M)(\rho \cos \phi, \rho \sin \phi) = u_m(\rho) \exp(m\phi)$ , the coefficients  $d_{j,l}$  must vanish unless  $j - 2l = m$ , so

$$u_m(\rho) = \sum_{l \geq 0, m+2l \leq k} d_{m+2l, l} \rho^{m+2l} + o(\rho^k) \quad \text{as } \rho \rightarrow 0.$$

This shows that  $u$  is  $k$ -times differentiable at  $P_+$  if and only if  $u_m$  satisfies the conditions (ii) and (iii) at  $\theta = 0$ . Writing derivatives of  $u$  of order  $\leq k$  in terms of derivatives of  $u_m$ , we see these derivatives are continuous if  $u_m \in C^k([0, \pi])$ . The argument for the pole  $P_-$  is analogous, with replacing the map  $M$  by  $-M$ .  $\square$

With the help of the following lemma, it can be shown that classical solutions to (9) are also weak solutions:

**Lemma 18.** *For all  $m \in \mathbb{Z}$  the operator  $\Delta_m^2$  is symmetric on the set*

$$\{u \in C^4([0, \pi]) : \Gamma_m u = 0, \Delta_m^2 u \in L^2([0, \pi], r^2 \sin)\} \subset L^2([0, \pi], r^2 \sin).$$

*Proof.* Recalling the separated Laplacian in (54) and the weighted  $L_\diamond^2$ -inner product allow us to perform the integration by part as

$$\begin{aligned}\langle \Delta_m^2 u, v \rangle &= -\langle \mathbf{grad}_h \Delta_m u, \mathbf{grad}_h v \rangle + [\sin \theta \partial_\theta (\Delta_m u) \bar{v}]_{\theta \rightarrow 0}^{\theta \rightarrow \pi} \\ &= \langle \Delta_m u, \Delta_m v \rangle + [\sin \theta \partial_\theta (\Delta_m u) \bar{v} - \sin \theta \Delta_m u \partial_\theta \bar{v}]_{\theta \rightarrow 0}^{\theta \rightarrow \pi} \\ &= \langle \Delta_m u, \Delta_m v \rangle + \frac{1}{r^2} \sum_{j=1}^5 [a_j(\theta)]_{\theta \rightarrow 0}^{\theta \rightarrow \pi} + \frac{m^2}{r^2} \sum_{j=1}^3 [b_j(\theta)]_{\theta \rightarrow 0}^{\theta \rightarrow \pi}\end{aligned}$$

with

$$\begin{aligned}a_1 &= -\cos \theta \partial_\theta u \partial_\theta \bar{v}, & a_2 &= -\sin \theta \partial_\theta^2 u \partial_\theta \bar{v}, & a_3 &= -\frac{1}{\sin \theta} \partial_\theta u \bar{v}, & a_4 &= \cos \theta \partial_\theta^2 u \bar{v}, \\ a_5 &= \sin \theta \partial_\theta^3 u \bar{v}, & b_1 &= \frac{-1}{\sin \theta} \partial_\theta u \bar{v}, & b_2 &= \frac{2 \cos \theta}{\sin^2 \theta} u \bar{v}, & b_3 &= \frac{1}{\sin \theta} u \partial_\theta \bar{v}\end{aligned}$$

for  $u, v \in H_\diamond^s(r\mathbb{S}^2)$ . Denoting the poles by  $p \in \{0, \pi\}$  and considering  $v$  having the same boundary conditions as  $u$ , we can see as follows that the boundary terms vanish for all  $m \in \mathbb{Z}$ :

$|m| \geq 2$ : Here  $u(p) = u'(p) = 0 = v(p) = v'(p)$  such that the limits for all the  $a_j$ -terms vanish. Moreover, we observe from l'Hospital's rule that  $\lim_{\theta \rightarrow p} b_2(\theta) = 2u'(p)\bar{v}'(p) = 0$  and  $\lim_{\theta \rightarrow p} b_j(\theta) = 0$  for  $j \in \{1, 3\}$  such that all  $b_j$ -limits vanish.

$|m| = 1$ : Here  $u(p) = u''(p) = 0 = v(p) = v''(p)$ , and hence  $\lim_{\theta \rightarrow p} a_j(p) = 0$  for  $j \in \{2, 4, 5\}$ . Moreover,  $\lim_{\theta \rightarrow p} (a_1 + a_3)(\theta) = -2 \cos(p)u'(p)\bar{v}'(p) = -\lim_{\theta \rightarrow p} b_2(\theta)$ , and  $\lim_{\theta \rightarrow p} (b_1 + b_3)(\theta) = 0$  by l'Hospital.

$m = 0$ : Here  $u'(p) = u'''(p) = 0 = v'(p) = v'''(p)$ , and we only need to discuss the  $a_j$ -terms, which vanish in the limit  $\theta \rightarrow p$  for  $j \in \{1, 2, 5\}$ . Moreover, by l'Hospital  $\lim_{\theta \rightarrow p} a_3(\theta) = -\cos(p)u''(p)\bar{v}(p) = -\lim_{\theta \rightarrow p} a_4(p)$ .  $\square$

*Remark 19* (Restricted domain – Cauchy boundary). It is clear that on the restricted domain  $I'$  as in Section 3.5 with boundary points  $p \in \partial I' = \{\epsilon, \pi - \epsilon\}$ , the symmetry property remains valid with Cauchy boundary conditions  $u(p) = u'(p) = 0$ .

## References

- [1] C. Aarset, M. Holler, and T. T. N. Nguyen. “Learning-informed parameter identification in nonlinear time-dependent PDEs”. In: *Applied Mathematics and Optimization* 88 (2023), 53 pp. DOI: 10.1007/s00245-023-10044-y.
- [2] R. A. Adams. *Sobolev Spaces*. New York: Academic Press, 1975.
- [3] N. Badr et al. “Algebra properties for Sobolev spaces - applications to semilinear PDEs on manifolds”. In: *JAMA* 118 (2012), pp. 509–544. DOI: 10.1007/s11854-012-0043-1.
- [4] S. Basu. “Global seismology of the Sun”. In: *Living Reviews in Solar Physics* 13.1, 2 (Aug. 2016), p. 2. DOI: 10.1007/s41116-016-0003-4. arXiv: 1606.07071 [astro-ph.SR].

- [5] Y. Bekki, R. H. Cameron, and L. Gizon. “Theory of solar oscillations in the inertial frequency range: Amplitudes of equatorial modes from a nonlinear rotating convection simulation”. In: *Astronomy & Astrophysics* 666, A135 (Oct. 2022), A135. DOI: 10.1051/0004-6361/202244150. arXiv: 2208.11081 [astro-ph.SR].
- [6] Y. Bekki, R. H. Cameron, and L. Gizon. “Theory of solar oscillations in the inertial frequency range: Amplitudes of equatorial modes from a nonlinear rotating convection simulation”. In: *Astronomy & Astrophysics* 666, A135 (Oct. 2022), A135. DOI: 10.1051/0004-6361/202244150. arXiv: 2208.11081 [astro-ph.SR].
- [7] L. J. Campbell. “Nonlinear dynamics of Rossby waves in a western boundary current”. In: *Advances in Fluid Mechanics VI* 52 (2006), pp. 457–468. DOI: 10.2495/AFM06045.
- [8] J. Christensen-Dalsgaard et al. “The Current State of Solar Modeling”. In: *Science* 272.5266 (1996). 10.1126/science.272.5266.1286, pp. 1286–1292. ISSN: 0036-8075.
- [9] T. G. Cowling. “The non-radial oscillations of polytropic stars”. In: *Monthly Notices of the Royal Astronomical Society* 101 (Jan. 1941), p. 367. DOI: 10.1093/mnras/101.8.367.
- [10] M. Eller, R. Griesmaier, and A. Rieder. “Tangential Cone Condition for the Full Waveform Forward Operator in the Viscoelastic Regime: The Nonlocal Case”. In: *SIAM Journal on Applied Mathematics* 84.2 (2024), pp. 412–432. DOI: 10.1137/23M1551845. eprint: <https://doi.org/10.1137/23M1551845>. URL: <https://doi.org/10.1137/23M1551845>.
- [11] L. C. Evans. *Partial Differential Equations*. Graduate Studies in Mathematics 19. AMS, Providence, RI, 1998.
- [12] D. Fournier, L. Gizon, and L. Hyest. “Viscous inertial modes on a differentially rotating sphere: Comparison with solar observations”. In: *Astronomy & Astrophysics* 664, A6 (2022), 16 pp. DOI: 10.1051/0004-6361/202243473.
- [13] L. Gizon et al. “Meridional flow in the Sun’s convection zone is a single cell in each hemisphere”. In: *Science* 368.6498 (June 2020), pp. 1469–1472. DOI: 10.1126/science.aaz7119.
- [14] L. Gizon et al. “Solar Inertial Modes”. In: *Dynamics of Solar and Stellar Convection Zones and Atmospheres Proceedings IAU Symposium No. 365, A. V. Getling & L. L. Kitchatinov, eds.* 2024.
- [15] L. Gizon et al. “Solar inertial modes: Observations, identification, and diagnostic promise”. In: *Astronomy & Astrophysics* 652, L6 (2021), 22 pp. DOI: 10.1051/0004-6361/202141462.

- [16] M. Hanke, A. Neubauer, and O. Scherzer. “A convergence analysis of the Landweber iteration for nonlinear ill-posed problems”. In: *Numer. Math.* 72 (1995), pp. 21–37.
- [17] E. Hebey. *Sobolev Spaces on Riemannian Manifolds*. Springer Berlin, Heidelberg, 1996. ISBN: 978-3-540-69993-4. DOI: 10.1007/BFb0092907.
- [18] H. Hoffmann, A. Wald, and T. T. N. Nguyen. “Parameter identification for elliptic boundary value problems: an abstract framework and application”. In: *Inverse Problems* 38.7 (2022), 44 pp. DOI: 10.1088/1361-6420/ac6d02.
- [19] S. Hubmer and R. Ramlau. “Convergence analysis of a two-point gradient method for nonlinear ill-posed problems”. In: *Inverse Problems* 33.9 (2017), p. 095004. DOI: 10.1088/1361-6420/aa7ac7.
- [20] S. Hubmer et al. “Lamé Parameter Estimation from Static Displacement Field Measurements in the Framework of Nonlinear Inverse Problems”. In: *SIAM Journal on Imaging Sciences* 11.2 (2018). DOI: 10.1137/17M1154461.
- [21] Y. Jiang, G. Nakamura, and K. Shiota. “Levenberg–Marquardt method for solving inverse problem of MRE based on the modified stationary Stokes system”. In: *Inverse Problems* 37.12, 125013 (2021).
- [22] B. Kaltenbacher, A. Neubauer, and O. Scherzer. *Iterative Regularization Methods for Nonlinear Problems*. Radon Series on Computational and Applied Mathematics. Berlin, New York: de Gruyter, 2008.
- [23] B. Kaltenbacher, T. T. N. Nguyen, and O. Scherzer. *The tangential cone condition for some coefficient identification model problems in parabolic PDEs*. Springer, 2021, 121–163. DOI: 10.1007/10.1007/978-3-030-57784-1\_5.
- [24] B. Kaltenbacher. “Convergence guarantees for coefficient reconstruction in PDEs from boundary measurements by variational and Newton-type methods via range invariance”. In: *IMA Journal of Numerical Analysis* drad044 (2023). DOI: 10.1093/imanum/drad044.
- [25] S. Kindermann. “Convergence of the gradient method for ill-posed problems”. In: *Inverse Problems & Imaging* 11.4 (2017), pp. 703–720.
- [26] S. Kindermann. “On the tangential cone condition for electrical impedance tomography”. In: *Electronic Transaction on Numerical Analysis* 57 (2022), pp. 17–34.
- [27] B. Müller et al. “Quantitative passive imaging by iterative holography: The example of helioseismic holography”. In: 40(4) (2024). DOI: 10.1088/1361-6420/ad2b9a.

- [28] J. C. Nédélec. *Acoustic and Electromagnetic Equations: Integral Representations for Harmonic Problems*. New York: Springer, 2001.
- [29] A. Neubauer. “On Nesterov acceleration for Landweber iteration of linear ill-posed problems”. In: *Journal of Inverse and Ill-posed Problems* 25.3 (2017), pp. 381–390. DOI: 10.1515/jiip-2016-0060.
- [30] T. T. N. Nguyen. “Sequential bi-level regularized inversion with application to hidden reaction law discovery”. In: *Inverse Problems* 41.6 (2025). DOI: 10.1088/1361-6420/addf73.
- [31] T. T. N. Nguyen. “Bi-level iterative regularization for inverse problems in nonlinear PDEs”. In: *Inverse Problems* 40.4 (2024), p. 045020. DOI: 10.1088/1361-6420/ad2905. URL: <https://dx.doi.org/10.1088/1361-6420/ad2905>.
- [32] J. Philidet and L. Gizon. “Interaction of solar inertial modes with turbulent convection. A 2D model for the excitation of linearly stable modes”. In: *Astronomy & Astrophysics* 673 (2023), 19 pp. DOI: 10.1051/0004-6361/202245666.
- [33] M. Renardy and R. C. Rogers. *An Introduction to Partial Differential Equations*. Springer, 1992.
- [34] P. H. Scherrer et al. “The Helioseismic and Magnetic Imager (HMI) Investigation for the Solar Dynamics Observatory (SDO)”. In: *Solar Physics* 275.1-2 (Jan. 2012), pp. 207–227. DOI: 10.1007/s11207-011-9834-2.
- [35] O. Scherzer, B. Hofmann, and Z. Nashed. “Gauss-Newton’s methods for solving linear inverse problems with neural network coders”. In: *Sampl. Theory Signal Process. Data Anal.* 21.25 (2023). DOI: 10.1007/s43670-023-00066-6.
- [36] M. E. Taylor. *Partial Differential Equations I*. Springer New York, NY, 2011. ISBN: 978-1-4614-2726-1. DOI: 10.1007/978-1-4419-7055-8.
- [37] M. J. Thompson et al. “The Internal Rotation of the Sun”. In: *Annu. Rev. Astron. Astrophys.* 41 (2003), pp. 599–643. DOI: 10.1146/annurev.astro.41.011802.094848.
- [38] H. Triebel. *Interpolation theory, function spaces, differential operators*. Amsterdam ; New York : North-Holland Pub. Co., 1978.
- [39] A. Versypt and R. Braatz. “Analysis of Finite Difference Discretization Schemes for Diffusion in Spheres with Variable Diffusivity”. In: *Comput Chem Eng.* 71 (2014), pp. 241–252. DOI: 10.1016/j.compchemeng.2014.05.022.
- [40] M. Watson. “Shear instability of differential rotation in stars”. In: *Geophysical & Astrophysical Fluid Dynamics* 16.1 (1981), pp. 285–298. DOI: 10.1080/03091928008243663.

- [41] E. Zeidler. *Nonlinear Functional Analysis and Its Applications I: Fixed-point theorems*. New York: Springer-Verlag, 1986, pp. xxi+897. DOI: 10.1007/978-1-4612-4838-5. URL: <http://dx.doi.org/10.1007/978-1-4612-4838-5>.